CO_2 Capture from Waste-to-Energy Plants: Techno-Economic Assessment of Novel Integration Concepts of Calcium Looping Technology

Martin Haaf[1], Rahul Anantharaman[2], Simon Roussanaly[2] Jochen Ströhle[1*], Bernd Epple[1]

[1]*Institute for Energy Systems and Technology, Technische Universität Darmstadt, Otto-Berndt-Straße 2, 64287 Darmstadt, Germany*

[2]*SINTEF Energy Research, Sem Saelandsvei 11, NO-7465 Trondheim, Norway*

*Corresponding Author:
Jochen Ströhle, Institute for Energy Systems and Technology, Technische Universität Darmstadt
Otto-Berndt-Straße 2, 64287 Darmstadt, Germany
Tel.: +49 6151 / 16 23003
Fax: +49 6151 / 1622690
Email: jochen.stroehle@est.tu-darmstadt.de

This is an author generated postprint of the article "Haaf M., Anantharaman R., Roussanaly S., Ströhle J., Epple B., 2020. CO_2 Capture from Waste-to-Energy Plants: Techno-Economic Assessment of Novel Integration Concepts of Calcium Looping Technology. Resources, Conservation and Recycling, 162, 104973." Copyright 2020 Published by Elsevier B.V. The final publication is available at https://doi.org/10.1016/j.resconrec.2020.104973.

Abstract

In Waste-to-Energy (WtE) plants, municipal solid waste (MSW) is combusted while power and/or heat are produced. This approach will largely remain as a promising option to handle the MSW capacities in the future. Due to the organic waste fractions present in MSW, net negative CO_2 emissions are feasible when integrating carbon capture and storage (CCS) processes into WtE plants. The calcium looping (CaL) process represents one option to capture CO_2 from WtE plant exhaust gases. Hereby, CO_2 is separated by a circulating limestone-based sorbent being exposed to cyclic carbonation-calcination reaction regimes. Within this study, a techno-economic analysis of a CaL retrofit on a generic 60 MW_{th} WtE plant is conducted. The analysis considerers three different types of supplementary fuel for the CaL process, namely coal, natural gas (NG) and solid recovered fuel (SRF). Based on a detailed process model, economic key performance indicators were calculated by means of a bottom-up approach. Additionally, different heat integration concepts were proposed and assessed. The techno-economic results are discussed in comparison to a benchmark MEA scrubbing process. It was found that levelized cost of electricity increases quite significantly, which leads to cost of CO_2 avoidance

in the range of 119 EUR/$t_{CO2,av}$ (CaL-SRF) up to 288 EUR/$t_{CO2,av}$ (MEA). It is important to note, that the supply of negative CO_2 emissions from a CCS equipped WtE plant enables a cost-efficient solution to at the same time treat MSW in a carbon neutral way while clean heat and/or power as well as negative CO_2 emissions are delivered.

Keywords: carbon capture and storage (CCS), waste-to-energy (WtE) plants, calcium looping (CaL) process, CO_2 negative solution, bioenergy with carbon capture and storage (BECCS)

Symbols

A	cross-sectional area, m²
a	decay constant of the solid concentration in the lean region, 1/m
c^*_{CO2}	equivalent CO_2 concentration in the fluidized bed, mol/m³
$c_{CO2,out}$	CO_2 concentration at the outlet of the carbonator, mol/m³
CAC	cost of CO_2 avoided, EUR/$t_{CO2,av}$
E_{carb}	carbonator CO_2 absorption rate, %
e_{CO2}	specific CO_2 emission, kg_{CO2}/MWh_e
E_{tot}	total CO_2 capture rate, %
F_0	molar flow of fresh limestone, mol/s
F_{CO2}	molar flow of CO_2 in the flue gas, mol/s
F_R	Ca-species circulating to the carbonator, mol/s
G^*_S	saturated solid mass flow in a riser, kg/m²s
H	height, m
HR_{CaL}	calcium looping heat ratio, -
k	deactivation constant of a sorbent particle, -
k_S	intrinsic kinetic constant of the carbonation reaction, $m^4/mols$
$LCOE$	levelized cost of electricity, EUR/MWh_e
M	molar mass, kg/kmol
N	number of complete carbonation-calcination cycles, -
PR_{CaL}	calcium looping gross power ratio, -
P_{th}	thermal power, MW_{th}
$r_{N,age}$	fraction of sorbent particles having N carbonation-calcination cycles, -
r_{CO2}	specific CO_2 mass flow, kg_{CO2}/MWh_e
$SPECCA$	specific primary energy consumption per CO_2 avoided, $MJ_{th}/kg_{CO2,av}$
T	temperature, °C
t	time, s

t_{lim}	time required for a sorbent particle to reach its maximum carbonation, s
u_0	superficial gas velocity, m/s
u_t	terminal particle velocity, m/s
x	molar fraction, -
X_{ave}	average carbonation degree of lime, -
$X_{max,ave}$	maximum average carbonation degree of lime, -
$X_{max,N}$	conversion capacity of a sorbent particle after N cycles, -
X_r	residual conversion capacity of a sorbent particle, -

Greek letters

ε	solid volume fraction in a fluidized bed, -
ε_{sd}	solid volume fraction in the dense phase of a fluidized bed, -
ε_{se}	solid volume fraction at the top of a fluidized bed, -
η	efficiency, %
ρ	mass density, kg/m³

Abbreviations

ASU	air separation unit
BE	back-end heat integration
BECCS	bioenergy carbon capture and storage
CA	combustion air
CaL	calcium looping process
CAPEX	capital expenditure
CCS	carbon capture and storage
CEPCI	chemical engineering plant cost index
CFB	circulating fluidized bed
DAC	direct air capture
DSI	dry sorbent injection
ECO	economizer
FW	feedwater
GPU	gas processing unit
HIC	heat integration concept
HP	high pressure
KPI	key performance indicator
LHV	lower heating value

LP	low pressure
MEA	monoethanolamine
MSW	municipal solid waste
NG	natural gas
NET	negative emission technology
OPEX	operational expenditure
RH	external reheating
SH	external superheating
SRF	solid recovered fuel
TCR	total capital requirement
TDC	total direct cost
TDCPC	total direct cost including process contingency
TRL	technology readiness level
TPC	total plant cost
WtE	waste-to-energy

Subscripts

0	fresh limestone
cal	calcium looping
calc	calciner
carb	carbonator
CCS	CCS system
d	dense region of a fluidized bed
e	electrical
g	gas phase
gross	gross electric efficiency, output
l	lean region of a fluidized bed
net	net electric efficiency/output
out	outlet
R	circulating Ca-species
Ref	reference system
s	solid phase
th	thermal
tot	total

1 Introduction

As a main outcome of the Paris Agreement in 2015, the goal to limit the global mean temperature increase by 2 °C or preferably 1.5 °C compared to pre-industrial levels was agreed on. Several global climate scenarios that provide possible pathways to achieve this goal rely on the large-scale removal of CO_2 from the atmosphere [1, 2]. Thus, negative emissions technologies (NETs) need to be deployed to achieve this goal. Examples of NETs include direct CO_2 air capture (DAC) [3, 4] and indirect CO_2 capture due to afforestation, ocean fertilization or algae culture [5]. Another possibility is the integration of carbon capture and storage (CCS) processes into industrial systems that emit a significant amount of biogenic CO_2 with their exhaust gases. This approach is typically referred to as bioenergy with CCS (BECCS) [6, 7]. Concerning the life cycle effects of a CCS process chain integrated into conventional power plants, the global warming potential decreases by up to 75 % [8]. However, several other environmental impact categories increase because of efficiency penalty, additional infrastructure and waste related to the capture process [9].

Municipal solid waste (MSW) represents a suitable fuel source for a BECCS system considering its large organic waste fractions. The generation of MSW is directly related to the growth rate of population and industrial activities. Thus, its generation is expected to grow from nearly 1.3 billion tons per year at present, to approximately 4.0 billion tons per year in 2025 [10]. Suitable waste treatment strategies are required in order to limit the pollution of the ecosystem and the emissions of greenhouse gases caused by improper waste disposal. The incineration of MSW in waste-to-energy (WtE) plants is a widely used waste treatment methodology. The main purpose of a WtE plant is the reduction of waste mass, volume and toxicity while generating power and/or heat by utilizing the energy chemically bound in the MSW as a useful byproduct [11]. Nearly 28 % of the MSW capacity in the EU-28 is treated by means of incineration [12]. Worldwide, approximately 750 WtE plants with a yearly MSW treatment capacity of almost 83 million tons are currently in operation [13]. The net electrical efficiency of a typical WtE is in the range of 10 - 30 % [14]. This relatively low value is caused by several reasons such as the low energy content of the raw MSW, its fluctuation in composition and size as well as the various corrosive species contained in the MSW reducing the effectiveness of heat recovery. Combustion systems for MSW, such as moving grates or fluidized beds, are specifically designed to guarantee a stable plant operation, complete fuel burnout along with non-toxic emissions rather than aiming at maximum boiler efficiency. The power cycle of a WtE plant is exposed to multiple corrosion phenomena, such as high temperature corrosion, molten salt corrosion, fouling and the erosion of heat exchanger surfaces

[15, 16]. In order to reduce the high temperature corrosion induced material losses to an acceptable value, the temperature of the superheated steam is often limited to approximately 400 °C [17]. A WtE plant represents a highly case specific system that is tailored to fit in the prevailing boundary conditions, such as local stack emissions limits, fuel composition, and the desired output product such as power and/or heat typically supplied as low pressure steam [18]. MSW or non-hazardous industrial wastes are often pre-processed and upgraded prior to combustion of the raw material [19]. The so-called solid recovered fuel (SRF) is classified according to crucial criteria such as maximum particle size, heating value or the content of chlorine and mercury [20]. Therefore, the combustion and heat recovery system for SRF are more efficient compared to the units that burn unclassified raw wastes. The utilization of SRF in CCS processes is beneficial due to the organic waste fractions and their relatively low or even negative fuel prices [21].

WtE plants represents a stationary CO_2 emitter that is reasonably large for the implementation of efficient CCS processes. Thereby, the benefits of an efficient MSW treatment and the achievement of negative CO_2 emissions are combined. Additionally, major disadvantages of BECCS applications based on cultivated energy crops, such as land system change, biosphere integrity or freshwater use are avoided, once the already available MSW is used as the biogenic carbon source [22]. In a recent study, it was found that a net removal of approximately 2.8 billion tons of CO_2 per year is globally feasible by 2100, assuming a comprehensive MSW treatment in WtE-CCS plants [23].

The calcium looping (CaL) process, represents one option for post-combustion CO_2 capture from WtE plants. The CaL process is particularly suited for being retrofitted to already existing industrial plants, such as power, cement, and WtE plants. The process makes use of the reversible carbonation-calcination reaction of limestone (Eq. 1).

$$CaO_{(s)} + CO_{2(g)} \leftrightarrow CaCO_{3(s)};\ \Delta H = \pm 178.2\ kJ/mol \tag{1}$$

Shimizu et al. [24] initially proposed the principle of the CaL process for CO_2 capture from coal-fired power plants. Figure 1 shows a schematic of the CaL process. The CaL process is one of the more advanced CO_2 capture processes under development and is currently at a technology readiness level (TRL) of 6 [25].

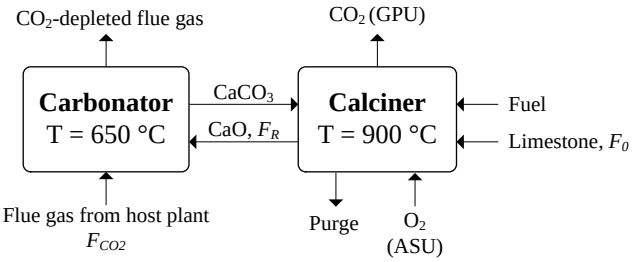

Figure 1: Schematic of the CaL process.

In this process, a limestone-based sorbent stream circulates between two interconnected fluidized bed reactors. The flue gas of the host plant is fed to the first reactor, the carbonator, where CO_2 reacts exothermically with calcium oxide (CaO) forming calcium carbonate ($CaCO_3$). The partly carbonated sorbent is subsequently transported to the second reactor, the calciner, where the temperature of the sorbent is raised to reach calcination conditions. Consequently, $CaCO_3$ decomposes to CaO and CO_2. Typically, the carbonator operates at approximately 650 °C, whereas close to 900 °C are required to ensure the complete calcination of the circulating sorbent in the calciner. The regenerated sorbent is recycled back to the carbonator to start the loop again. In the most mature CaL process configuration, the required heat for the calciner is supplied by means of oxy-fuel combustion of supplementary fuel. In the proposed concept, an on-site cryogenic air separation unit (ASU) supplies the required technically pure oxygen. The highly concentrated CO_2 stream available at the outlet of the calciner needs to be further purified and compressed in a gas processing unit (GPU) in order to fulfill the requirements for the subsequent transportation, long-term storage or utilization. To account for the deactivation of the circulating sorbent, a constant flux of fresh limestone is fed to the process, while ashes and deactivated sorbent are discharged [26]. The performance characteristics within a CaL system are commonly described by the molar flows of the main material streams in the system (see Figure 1). Namely, the molar flow of CO_2 that is fed to the carbonator with the flue gas of the host unit, F_{CO2}, the molar flow of Ca-species that circulates between calciner and carbonator, F_R, and the molar flow of fresh limestone contained in the make-up that is introduced to the system, F_0. One key metric within the CaL process is the CO_2-absorption efficiency within the carbonator, E_{carb} according to Eq. 2.

$$E_{carb} = \frac{F_{CO2,abs}}{F_{CO2}} = \frac{F_{CO2} - F_{CO2,carb,out}}{F_{CO2}} \tag{2}$$

Here, $F_{CO2,abs}$ is the molar flow of CO_2 that is absorbed by CaO in the carbonator and, $F_{CO2,carb,out}$ states the molar flow of CO_2 at the outlet of the carbonator. Due to the very high

CO_2 capture ratio of the oxy-fuel fired calciner, the CO_2 released during the combustion of the supplementary fuel, $F_{CO2,fuel}$, and the CO_2 released by the first calcination of the fresh limestone, F_0, are nearly completely captured. Thus, the total CO_2 capture rate of the CaL process, E_{tot} is further increased:

$$E_{tot} = \frac{F_{CO2,capt}}{F_{CO2,in}} = \frac{F_{CO2,calc,out}}{F_{CO2} + F_{CO2,fuel} + F_0} \quad (3)$$

Within the past years, continuous CO_2 capture by means of the CaL process has been successfully demonstrated in various test rigs up to megawatt scale. The development of the CaL process is boosted by similarities between the CaL CFB reactors and the already well-understood fundamentals of CFB boilers. Experimental results were reported from several small-scale units (< 300 kW_{th}) [27-30] and large-scale units (> 1000 kW_{th}) such as the 1 MW_{th} pilot plant at Technische Universität Darmstadt (Germany) where the unit has been in continuous operation for 1,200 h using hard coal and lignite as supplementary fuel [31, 32]. The operation of an SRF-fired CaL process has been successfully demonstrated at same unit [33, 34]. Other large-scale units are the 1.7 MW_{th} pilot plant in La Pereda (Spain) [35], and the largest CaL pilot plant (1.9 MW_{th}) in Hsinchu (Taiwan) [36].

Due to the relatively high operation temperatures of the CaL process (T_{carb} = 650 °C, T_{calc} = 900 °C), efficient recovery of excess heat by means of a dedicated supercritical water-steam cycle is feasible. The heat demand of the calciner represents one key thermodynamic metric of a CaL system. This parameter is mainly influenced by the required make-up flow and solid circulation rate needed to achieve the desired CO_2 absorption efficiency in the carbonator. Thus, there are several models published in literature that focus on carbonator and sorbent deactivation modelling [37]. For full-scale state-of-the-art coal-fired power plants, several research groups have calculated the net electrical efficiency drop to the range of 5 to 8 %-points (including the power demand of the CO_2 compression) by means of process simulations [38-40]. The corresponding costs of CO_2 avoidance range from 25 up to 50 EUR/$t_{CO2,av}$ [8, 41]. Until now, no techno-economic evaluation of the CaL process in the framework of WtE plants has been performed.

In this study, a generic WtE plant retrofitted with the CaL process for CO_2 capture is assessed by means of a techno-economic analysis. Based on a detailed CaL process model, the investment costs of equipment are calculated using a bottom-up approach. Coal, natural gas (NG) and SRF are considered as supplementary fuels for the calciner. Subsequently, levelised cost of electricity (LCOE) and cost of CO_2 avoidance (CAC) are calculated. In addition to the

techno-economic discussion of a standard back-end integration case, the effects of the CaL process conditions and- CaL power cycle parameter were assessed thermodynamically. Moreover, a concept with tight heat integration between WtE plant and CaL process is proposed and discussed where WtE live steam is superheated externally utilizing excess heat from the CaL process.

2 Methodology

2.1 Reference WtE plant

A generic 60 MW_{th} WtE plant based on a moving grate combustion system for MSW with an average lower heating value (LHV) of 10 MJ/kg serves as a reference for this study. The elementary composition of the MSW is given in Table 3 (Appendix). The heat recovery system delivers superheated steam at 40 bar and 400 °C to the inlet of the steam turbine. Figure 9 (Appendix) shows the thermodynamic power cycle layout. Table 4 (Appendix) summarizes the boundary conditions of the reference WtE plant. The steam turbine is equipped with three steam bleedings for preheating of the combustion air and for condensate preheating, respectively. The flue gas cleaning system consists of a dry sorbent injection (DSI) unit to meet the stack emission limits. The composition of the WtE flue gas at the interface to the CaL process is summarized in Table 5 (Appendix). The total specific CO_2 emissions of WtE plant accumulate to 1684 g_{CO2}/kWh_e, whereof the fossil CO_2 emissions (590 g_{CO2}/kWh_e) are significantly lower due to the organic waste fractions.

2.2 Process Modelling

2.2.1 CaL Process

The thermodynamic modelling of the CaL process and the connected heat recovery system is carried out in the ASPEN PLUS 8.8® flowsheet simulation environment, using the Peng Robinson equation of state. A simplified process flowsheet of the CaL unit including the heat recovery system is shown in Figure 2. The main modeling assumptions are summarized in Table 7 (Appendix). The solid looping systems consist of the carbonator and the calciner, each equipped with a cyclone. The calciner is modelled according to the approach of the Gibbs free energy minimization, assuming isothermal conditions. The specific sorbent circulation rate (F_R/F_{CO2}) is kept constant, whereas the specific make-up rate (F_0/F_{CO2}) is varied in order to achieve the desired CO_2 absorption efficiency within the carbonator. In order to account for the different ash properties of SRF and coal, cyclone separation efficiencies are altered according to the type of fuel that is utilized (see Table 7). After each CFB reactor, heat is recovered from

hot gas streams within a convective pass. In order to minimize the risk of high-temperature corrosion in the case of SRF-firing, the arrangement of the convective heat exchanger surfaces is modified compared to Figure 2. Accordingly, the hot CO_2 product stream at the calciner outlet is cooled by means of evaporator tubes (EVA 2) before it is used to feed the first steam superheater (SH 1). In addition to that, a chlorine removal unit is foreseen downstream of the calciner convective pass in the case of firing with SRF. After each convective heat transfer section, bag filters separate the remaining fly ash before the gases are further cooled down in the condensate preheating section. Part of the calciner off-gas is recirculated back to the inlet of the calciner for dilution of the oxygen. The fresh limestone and the supplementary fuel are fed directly to the calciner. The oxygen delivered by the ASU is preheated by the purge material. Table 3 (Appendix) and Table 6 (Appendix) summarize the elementary analysis and LHV of the solid fuels, and NG.

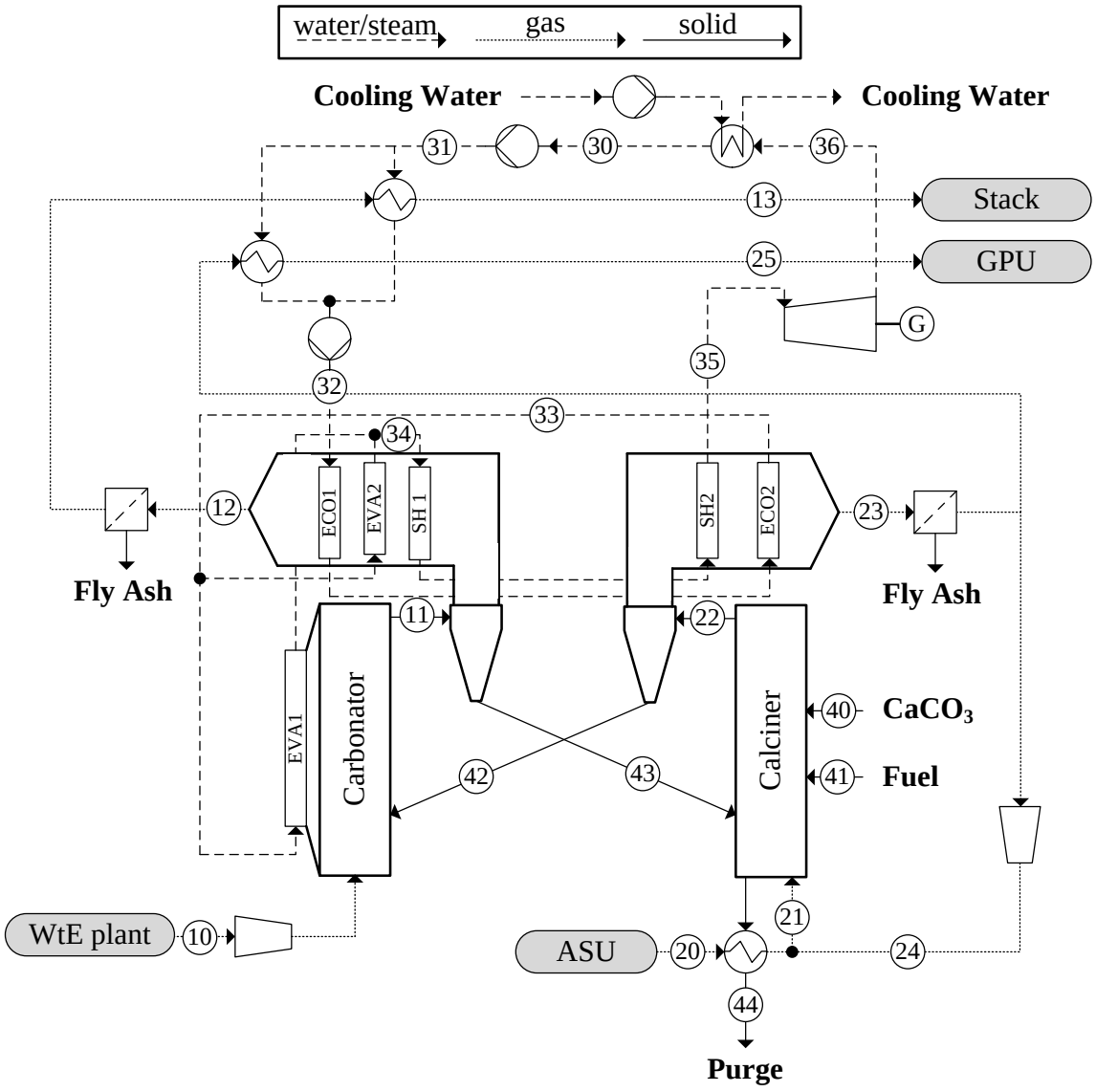

Figure 2: Model flowsheet of the CaL solid looping and heat recovery system.

Within the CaL process, the deactivation of the circulating sorbent and the related CO_2 absorption efficiency within the carbonator are key parameters. Thus, a detailed sequence for the calculation of the carbonator performance is implemented in the flowsheet simulation via a FORTRAN interface. The solid distribution within the carbonator riser is calculated with an empirical approach from Kunii and Levenspiel [42-44]. Accordingly, the carbonator riser is distinguished into a dense phase in the lower part of the reactor and the upper lean phase while in parallel a core and a wall zone is considered. The dense phase has a constant volumetric particle concentration, (ε_{sd} = 0.16), whereas the solid population in the lean phase decreases exponentially according to the decay constant, a. The decay constant is dependent on the superficial gas velocity, u_0, such that au_0 = 3. The volumetric concentration of solid at the riser outlet, ε_{se} is calculated according to Eq. 4.

$$\varepsilon_{se} = \varepsilon_s^* + (\varepsilon_{sd} - \varepsilon_s^*)\varepsilon^{-aH_l} \tag{4}$$

Where H_l is the height of the lean phase. The saturated capacity of the gas, ε_s^*, can be derived from Eq. 5, where G_s^* is the saturated mass flow of solid, u_t is the terminal velocity of the particles, and ρ_s is the mass density of the solid.

$$\varepsilon_s^* = \frac{G_s^*}{(u_0 - u_t)\rho_s} \tag{5}$$

The saturated mass flow is calculated with a correlation of Geldart et al. [45] according to Eq. 6.

$$G_s^* = 23{,}7\rho_g u_0 e^{-\frac{5.4u_t}{u_0}} \tag{6}$$

The total solids inventory is then derived from the sum of solid hold up in the lean and dense phase according to Eq. 7.

$$W = A\rho_s H_d \varepsilon_{sd} + A\rho_S H_l \overline{f_l} \tag{7}$$

Here, A is the cross-sectional area of the carbonator, H_d states the height of the dense phase and, $\overline{f_l}$ states the average volumetric particle concentration in the lean phase (Eq. 8).

$$\overline{f_l} = \varepsilon_s^* + \frac{\varepsilon_{sd} - \varepsilon_{se}}{H_l a} \tag{8}$$

The CO_2 absorption efficiency within the carbonator is calculated using the model of Romano [46]. This model has been validated by means of experimental data obtained in two different CaL test facilities [46, 47].

The evolution of the CO_2 carrying capacity of the sorbent is determined depending on the deactivation constant, *k*, and the residual conversion capacity, X_r, as proposed by Grasa and Abanades [48]:

$$X_{max,N} = \frac{1}{\frac{1}{1 - X_r} + kN} + X_r \tag{9}$$

In this work, the values chosen for the deactivation constant and the residual conversion capacity without sulfation are 0.52 and 0.075 respectively. *N* represents the numbers of complete calcination/carbonation cycles.

The degree of sulfation of the sorbent has a significant influence on the evolution of the CO_2 carrying capacity of the limestone due to the blockage of particle pores [49]. Sulfur species are introduced into the CaL system by the flue gas from the WtE plant that is fed to the carbonator and by the sulfur present in the supplementary fuel that is burnt in the calciner. An appropriate flue gas cleaning system limits the first proportion, whereas the second proportion can be limited by an appropriate choice of fuel. Calcium sulfate ($CaSO_4$) that is formed either directly (Eq. 10) or indirectly (Eq. 11) remains stable under typical CaL process conditions [50].

$$CaCO_{3(s)} + SO_{2(g)} + \frac{1}{2} O_{2(g)} \rightarrow CaSO_{4(s)} + CO_{2(g)} \tag{10}$$

$$CaO_{(s)} + SO_{2(g)} + 0.5 O_{2(g)} \rightarrow CaSO_{4(s)} \tag{11}$$

To account for the sulfur induced sorbent deactivation, the deactivation constant and the residual conversion capacity of the sorbent are calculated depending on the molar sulfating level of the sorbent, x_{CaSO4} . For this purpose, experimental data from Grasa et al. [51] are applied to the empirical Eqs. 12 to 14.

$$k_r = k_{r,0}(1 + 0.2962 * x_{CaSO4}) \tag{12}$$

$$X_r = X_{r,0}(1 - 1.1536 * x_{CaSO4}), for\ x_{CaSO4} \leq 0.5 \quad (13)$$

$$X_r = X_{r,0}(0.4230 - 3.076 * x_{CaSO4}), for\ x_{CaSO4} > 0.5 \quad (14)$$

The calculation of the CO_2 absorption efficiency within the carbonator is conducted in terms of the sorbent molar conversion and the material balance, respectively. The first approach takes into account the average maximum conversion, $X_{max,ave}$, of the sorbent particles:

$$X_{max,ave} = \sum_{N=1}^{+\infty} r_N X_{max,N} \quad (15)$$

Here, r_N, is the age structure of the particles. It is dependent on the number of complete carbonation-calcination cycles, N, and the real level of carbonation (f_{carb}) and calcination (f_{calc}) [52].

The average conversion degree of the particles, X_{ave}, is determined according to Eq. 16. The average conversion of particles with a residence time greater than t_{lim} is equal to the maximum conversion at the end of the fast reaction stage, X_N. For particles having a residence time smaller than t_{lim}, the average conversion is a function of a given CO_2 concertation, c^*_{CO2} and the number of complete carbonation-calcination cycles.

$$X_{ave} = \sum_{N=1}^{+\infty} r_N \left(\int_0^{t_{lim}} f(t) X(t, N, c^*_{CO2}) dt + \int_{t_{lim}}^{\infty} f(t) X_{max,N} dt\right) \quad (16)$$

The CO_2 absorption efficiency, according to the sorbent molar conversion, $E_{carb,I}$, is then obtained by Eq. 17 and the given molar flows of CaO and CO_2 entering the carbonator.

$$E_{carb,I} = \frac{F_R X_{ave}}{F_{CO2}} \quad (17)$$

The calculation sequence for the CO_2 absorption efficiency depends on the material balance, $E_{carb,II}$, based on the reaction constant, k_{ri}, according to Eq. 18 [53].

$$k_{ri} = \frac{\rho_{s,a}}{M_{s,a}} \sum_{N_{age}=1}^{\infty} r_{N,age} \int_0^{t_{lim}} f(t)\, k_s S_N (1 - X(t, N_{age}, c^*_{CO2}))^{2/3} dt \quad (18)$$

Here, k_s, is the intrinsic kinetic constant of the carbonation reaction set as 6.05 * 10^{-10} m^4/mols, S_n is the specific surface area of CaO-particles having N calcination-carbonation cycles, and c^*_{CO2} states the given CO_2 concentration. The amount of CO_2 being absorbed in the carbonator riser is then calculated according to the K-L model. The overall CO_2 absorption efficiency according to the material balance is finally derived from Eq. 19 [46].

$$E_{carb,II} = \frac{F_{CO2} - \dot{V}_{g,out} * c_{CO2,out}}{F_{CO2}} \quad (19)$$

Here, $\dot{V}_{g,out}$ is the volumetric flow rate of flue gas at the outlet of the carbonator, and $c_{CO2,out}$ is the CO_2 concentration at the carbonator outlet. If the difference between, $E_{carb,I}$ and $E_{carb,II}$ is reasonable small (< 0.005), the average value of both numbers is applied. Otherwise, the initial start value of c^*_{CO2} is adjusted iteratively.

2.2.2 Gas Processing Unit

A single stage flash, self-refrigerated GPU suitable for pipeline transport of CO_2 is used to purify the CO_2-rich stream from the calciner after heat integration. The desired outlet pressure of the CO_2-product is 110 bar at a purity of 96 % (T < 30 °C) according to common specification for CO2 pipeline transport [54, 55]. A schematic of the GPU is shown in Figure 11 (Appendix). The CO_2 stream after the condenser is compressed to specified pressure depending on the CO_2 capture ratio required. This stream is then dried using molecular sieves. This dry gas is cooled down to -50 °C in a multi-stream heat exchanger to liquefy the CO_2 and separate it from the impurities such as nitrogen and oxygen. The CO_2 liquid is flashed to reduce the temperature to -54 °C. The liquid CO_2 (before flashing), the vapor CO_2 (after) flashing) and the N_2-rich vent streams are used to cool down the feed gas to the GPU in the multistream heat exchanger. The minimum temperature difference between hot and cold composite curves in the multistream heat exchanger is set to 3 K. The process can be optimized by varying the separator pressure and keeping the pressure at the outlet of the throttle as high as possible without violating the minimum temperature difference in the multistream heat exchanger.

2.2.3 MEA-Absorption Process

Reactive CO_2 absorption with aqueous amine solutions as solvent is considered as the most mature option for CO_2 capture. Absorption with amine is the technology used at the first full

scale CO_2 capture power plant in Boundary Dam in Canada [56, 57]. Absorption with aqueous solution of monoethanolamine (MEA) is established as reference technology in benchmark studies of CO_2 capture processes.

The principle of the technology is shown in Figure 10 (Appendix). The solvent (30 wt.% MEA) is circulated between an absorber and a desorber. Flue gas is sent through the absorber, where the CO_2 reacts with MEA and is dissolved in the solvent. The CO_2 rich solvent is heated and sent to the desorber. In the desorber the solvent is regenerated by further heating with a reboiler operated at approximately 120 °C. The reaction is reversed, and CO_2 is released from the solvent. The desorber is operated at a pressure of 1-2 bars, which means that the purified CO_2 is produced at this pressure. It is sent to further conditioning for transport and storage/reuse by compression or liquefaction. The CO_2 lean solvent is recirculated back to the absorber.

MEA can separate CO_2 at very low partial pressures, and the CO_2 is produced at high purity. However, it requires high thermal energy for regeneration, it is corrosive, and the amine degrades over time [58]. In this study, the specific heat consumption of 3.9 MJ_{th}/kg_{CO2} is assumed for 90 % CO_2 capture from the WtE flue gas. This heat will be supplied by steam extraction at 4 bar. Moreover, the auxiliary power demand is 0.432 MJ_e/kg_{CO2}.

2.3 Cost Evaluation Methodology

This section presents the cost assessment methodology considered for the evaluation of the CO_2 capture and conditioning process and the evaluation of cost-related key performance indicators (KPI) for the WtE plant retrofitted with the CaL process. All cost numbers presented in this work are given in 2017 price level. Cost data is taken from literature and available in different years were updated to 2017 price level using cost indexes such as the Chemical Engineering Plant Cost Index (CEPCI) [59] or inflation [60]. This paper does not include a techno-economic evaluation of the WtE plant without CO_2 capture, therefore, a LCOE of 80 EUR/MWh_e is assumed here [61, 62].

2.3.1 Investment Costs

Figure 3 shows the adopted bottom-up applied in this study to assess the investment costs of the CO_2 capture processes. Accordingly, the equipment and direct costs of the different components of the capture process have been assessed following different methods: Aspen Process Economic Analyzer®, cost database, power law, quotations from vendor, etc. In particular, the equipment and direct cost of standard components (e.g. packed column, heat exchanger, compressors, pumps) are assessed using Aspen Process Economic Analyzer®, while the cost of non-standard components (e.g. carbonator, calciner, ASU) are assessed as

illustrated in Table 8 (Appendix) due to their specificity. Process contingencies are then added to the total direct cost (TDC) [63]. Indirect costs, and project contingencies are added to the TDC with process contingencies (TDCPC) to reach the total plant cost (TPC) [63, 64]. Process contingencies, *P1*, are set to 15 % of TDPC for the CO_2 conditioning step, whereas 32 % of TDPC are assumed for the CaL system due to the lower level of maturity [65]. Auxiliary system process contingencies are set to 5 % of TDCPC. Project contingencies, *P2*, for all subsystems are specified by 15 % of TDPC [66].

Finally, the owner costs and interest over construction are added to the TPC to calculate the total capital requirement (TPC). The owner cost are considered to represent 7% of TDCPC and the interest over construction are calculated assuming that the construction costs are shared over a three-year construction period following a 40/30/30 allocation [67].

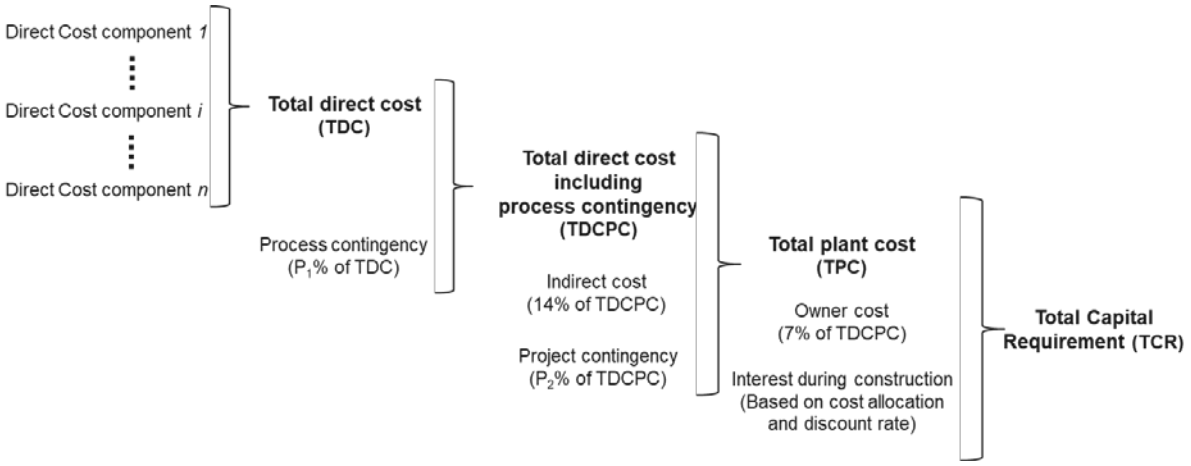

Figure 3: Illustration of the adopted bottom-up approach for evaluation of investment costs.

2.3.2 Operating Costs

Fixed operating costs cover maintenance, insurance and labour costs. The annual costs of preventive and corrective maintenance (2 %), insurance (2 %), and local taxes (0.5 %) are calculated as 4.5 % of the total plant cost [64]. Meanwhile, the labour cost composed of three components (operating labour, maintenance labour, and administrative labour) is derived as follows [67, 68]. The operating labor is estimated based on the expected number of employees to run the CO_2 capture process and a fully burdened annual cost of 60 k€ per employee. The maintenance labour is assumed to correspond to 40 % of the total maintenance annual cost. The administrative labour is assumed to be 30 % of the operating and maintenance labour cost. The annual variable operating costs of the CO_2 capture processes are evaluated based on utilities consumption obtained from the process design and the utilities cost shown in Table 9 (Appendix). While most of these costs are commonly used in literature, it is worth noting

that the SRF cost varies greatly in literature. As a consequence, two SRF cost scenarios are considered in this study: 10 and 25 EUR/t_{SRF} [68]. These numbers correspond to a production cost of 0 and 15 EUR/t and transport cost of 10 EUR/t_{SRF}.

2.4 Key Performance Indicators

For the evaluation and comparison of techno-economic process performance, the following KPI´s are introduced. The CaL process heat ratio, HR_{CaL}, refers to the share of the thermal input to the CaL process, $P_{th,CaL}$, on the total heat input to the system, $P_{th,tot}$ according to Eq. 20. $P_{th,tot}$ is derived from the sum of the heat input to the WtE plant, $P_{th,WtE}$, and to the CaL calciner.

$$HR_{CaL} = \frac{P_{th,caL}}{P_{th,tot}} = \frac{P_{th,CaL}}{P_{th,WtE} + P_{th,CaL}} \tag{20}$$

Similar to the CaL heat ratio, one can derive the CaL gross electrical ratio, PR_{CaL} according to Eq. 21. Here, $P_{el,CaL,gross}$ is the gross power output of the CaL water steam cycle, $P_{el,WtE,gross}$ is the gross power output of the WtE water steam cycle, and $P_{el,tot,gross}$ is the sum of CaL process and WtE plant gross power output.

$$PR_{CaL} = \frac{P_{el,CaL,gross}}{P_{el,tot,gross}} = \frac{P_{el,CaL,gross}}{P_{el,WtE,gross} + P_{el,CaL,gross}} \tag{21}$$

The specific CO_2 emissions of the WtE plant retrofitted by the CaL process, $e_{CO2,CaL}$, are calculated by Eq. 22. Thereby, $\dot{m}_{CO2,foss}$ is the mass flow of fossil CO_2 being emitted to the atmosphere, $\dot{m}_{CO2,capt,bio}$ is the mass flow of biogenic CO_2 being captured and, $P_{el,net}$ is the net power delivered by the total system.

$$e_{CO2,CCS} = \frac{\dot{m}_{CO2,foss} - \dot{m}_{CO2,capt,bio}}{P_{el,tot,net}} \tag{22}$$

In order to evaluate the energy performance of a CCS unit, the specific primary energy consumption per CO_2 avoided (SPECCA) is calculated. For CaL applications, the fact of the additional power supply by the CaL process needs to be considered. Accordingly, the calculation of the SPECCA can be described as follows:

$$SPECCA = \frac{\frac{1}{\eta_{net,CaL}} - \frac{1}{\eta_{net,Ref}}}{e_{CO2,Ref} - e_{CO2,CaL}} = \frac{\frac{1}{\eta_{net,CaL}} - [x_i * \frac{1}{\eta_{net,i}} + (1 - x_i)\frac{1}{\eta_{net,WtE}}]}{[(1 - x_i) * e_{CO2,Wte} + x_i * e_{CO2,i}] - e_{CO2,CaL}} \tag{23}$$

Hereby, $\eta_{net,CCS}$ is the net electrical efficiency of the WtE plant with CaL, and $\eta_{net,Ref}$ is the net electrical efficiency of the WtE plant without CaL while considering the efficiency of a state-of-the-art power plant for each type, i, of supplementary fuel. Moreover, $e_{CO2,WtE}$ is the specific fossil CO_2 emission of the reference WtE plant, $e_{CO2,i}$ is the specific CO_2 emission for the conversion of the type of fuel in state-of-the-art power plants. The specific CO_2 emissions and the net electrical efficiency of the reference system are weighted by the share, x_i, of the additional power that is supplied to the grid by the CaL unit. Table 10 (Appendix) summarizes the boundary conditions for the state-of-the-art power plants to calculate the reference state.

The LCOE measures the unit cost of a power plant, with and without CO_2 capture, and approximates the average discounted electricity price over the project duration that would be required as income to match the net present value of costs of the project. It is equal to the annualized costs divided by the annualized net electricity production, as shown in Eq. 24.

$$\mathrm{LCOE}_{\mathrm{CCS}} = \frac{LCOE_{\mathrm{Ref}} \cdot (\mathrm{MWh/y})_{\mathrm{ref}} + Annualised\ investment_{CCS} + Annual\ OPEX_{CCS}}{(\mathrm{MWh/y})_{\mathrm{CCS}}} \quad (24)$$

where

- $LCOE_{\mathrm{CCS}}$ is the LCOE produced by the plant with CO_2 capture
- $\mathrm{LCOE}_{\mathrm{Ref}}$ is the LCOE of the reference plant without CO_2 capture
- $(\mathrm{MWh/y})_{\mathrm{CCS}}$ is the annual electricity production of the plant with CO_2 capture
- $(\mathrm{MWh/y})_{\mathrm{ref}}$ is the annual electricity production of the plant without CO_2 capture
- $Annualised\ investment_{CCS}$ is the annualized investment cost of the CO_2 capture process
- $Annual\ OPEX_{CCS}$ is the annual operating cost of the CO_2 capture process

Similar to the technical evaluation of the reference state, the $LCOE_{Ref}$ needs to be modified according to the additional power that is produced by the CaL unit:

$$LCOE_{Ref} = (1\text{-}x) * LCOE_{WtE} + x * LCOE_i \quad (25)$$

Thereby, $LCOE_i$ states the LCOE for state-of-the-art power units for each type of supplementary fuel, respectively (see Table 10, Appendix).

The CAC, which is obtained by comparing the LCOE and the CO_2 emission rate to the atmosphere of the plant with and without CO_2 capture, shown in Eq. 26. The CAC approximates

the average discounted CO_2 credit (tax or quota) over the duration of the project that would be required as income to match the net present value of costs due to the CO_2 capture implementation.

$$CAC = \frac{LCOE_{\mathrm{CCS}} - LCOE_{\mathrm{Ref}}}{e_{\mathrm{CO2,Ref}} - e_{\mathrm{CO2,CCS}}} \tag{26}$$

LCOE and CAC are calculated assuming a real discount rate of 8 %[1]. An economic lifetime of 25 years and an average yearly utilization rate of 85 % are further assumed. The annualized investment are calculated assuming a fixed charge factor of 9.36 % based on the 8 % discount rate and 25 years of economic lifetime assumptions.

3 Performance Assessment of WtE plant with CO_2 capture

3.1 Thermodynamic Assessment of the Back-end integration

Relevant mass flows according the nomenclature given in Figure 2 are listed in the Tables 12 - 13 (Appendix) for each type of fuel, respectively. Table 1 summarizes relevant process performance parameters for each CCS option.

Table 1: Key results of the CaL process for the different CCS options[2].

Parameter	Unit	MEA	CaL		
			Coal	NG	SRF
Specific make-up feed (F_0/F_{CO2})	-	-	0.24	0.09	0.24
Specific circulation rate (F_R/F_{CO2})	-	-	10.0	10.0	10.0
CO_2 absorption rate (E_{carb})	%	-	80.0	80.0	80.0
Total CO_2 capture rate (E_{tot})	%	90.0	90.8	87.1	91.1
$CaCO_3$ content at carbonator outlet	wt.%	-	12.3	13.4	10.5
$CaSO_4$ content at calciner outlet	wt.%	-	2.82	0.51	2.45
Ash content at calciner outlet	wt.%	-	6.71	0.00	20.1
Oxygen flow to the calciner	kg/s	-	5.72	5.08	6.55
Calciner thermal input	MW_{th}	-	62.3	55.6	71.7
Carbonator cross section	m^2	-	19.2	19.2	19.2
Calciner cross section	m^2	-	8.9	8.5	11.5
CaL process heat ratio (HR_{CaL})	%	-	50.9	48.1	54.5
Gross power CaL power cycle	MW_e	-	16.9	15.7	19.4
CaL process gross power ratio (PR_{CaL})	%	-	51.9	50.0	55.2
CCS Auxiliary	MW_e	2.47	1.58	1.55	1.63
ASU power demand	MW_e	-	4.53	4.03	5.18
GPU power demand	MW_e	-	4.94	3.49	5.13
GPU specific power consumption	kJ_e/kg_{CO2}	-	392	396	395

[1] That corresponds to a nominal discount rate of approximately 10 % based on an inflation rate of 2 %.

[2] For the reference WtE plant heat input and net power see Table 4 (Appendix)

GPU CO_2 slip	%	-	2.08	3.30	2.97
Total net power output	MW_e	5.07	19.6	20.3	21.1
Total net electrical efficiency	%	9.64	16.0	17.6	16.0
Reference net electrical efficiency	%	22.4	29.7	34.5	23.6
SPECCA	$MJ_{th}/CO_{2,av}$	21.8	9.48	10.2	5.72

Thermodynamically, NG allows for the lowest CaL heat demand and the highest net electrical efficiency. This is mainly due to relatively low sulfur content and the absence of any fuel ash. When utilizing SRF or coal as supplementary fuels in the calciner, a higher flux of fuel-sulfur is introduced to the CaL-system. Accordingly, more make-up is needed to compensate for sorbent deactivation. Additionally, the accumulation of ashes in the circulating sorbent stream raises the thermal requirements of the calciner. The ash enrichment is even more of concern for SRF. In addition to the auxiliary power of the ASU and the GPU, the heat requirement for the first calcination of the fresh limestone represents a contributor to the electrical efficiency penalty, since this heat share cannot be recovered. While 4.2 % of the calciner heat input is consumed by the first calcination while firing NG, this number increases to 9.7 % and 8.5 % for the cases of coal and SRF, respectively. Among all cases, the CaL gross electrical ratio exceeds the CaL heat ratio. This is mainly justified by the more efficient layout of the CaL power cycle in comparison to the existing WtE power cycle. In the case of NG, almost 50 % of the total gross power is delivered by the CaL power cycle. The SPECCA for the coal and NG case are relatively high in comparison the corresponding value of SRF. This is partly due to the fact that the current large scale state-of-the-art net electrical efficiency of coal and NG power plants allows for a more efficient supply of electricity in comparison to typical SRF power plants. Thus, it could be stated that in terms of an efficient fuel utilization under the circumstances of WtE plants, the application of SRF is favorable.

The SPECCA for the MEA based capture process is higher than the values for the CaL process no matter which type of supplementary fuel is used. It should be noted that the energy penalty of the MEA process can be reduced through advanced heat integration through the use of heat pumps etc. Such advanced integration is not included as part of this work.

In addition to drop in the net electrical efficiency of the retrofitted WtE plant, the specific CO_2 avoidance is of concern. Figure 4 shows the specific CO_2 emissions, the derived specific CO_2 avoidance and the negative CO_2 emissions on a yearly basis for the MEA case and for different CaL fuel options. Table 14 (Appendix) summarizes the CO_2 mass flows within the CaL system that are applied here. The reference fossil CO_2 emission in the NG case shows the lowest specific CO_2 emissions due to the low carbon intensity of this type of fuel. When coal is used, the reference CO_2 emissions increase. In case of SRF, the specific CO_2 emissions in the reference state are governed by the low fuel reference net electrical efficiency and the organic

waste fractions. In case of the MEA process, reference CO_2 emissions are the same as for the WtE plant w/o CCS, since no additional electrical power is produced. The amount of negative CO_2 emissions shows the highest value in case of CaL-SRF, due to the large quantities of organic waste fractions additionally burned in the CaL calciner.

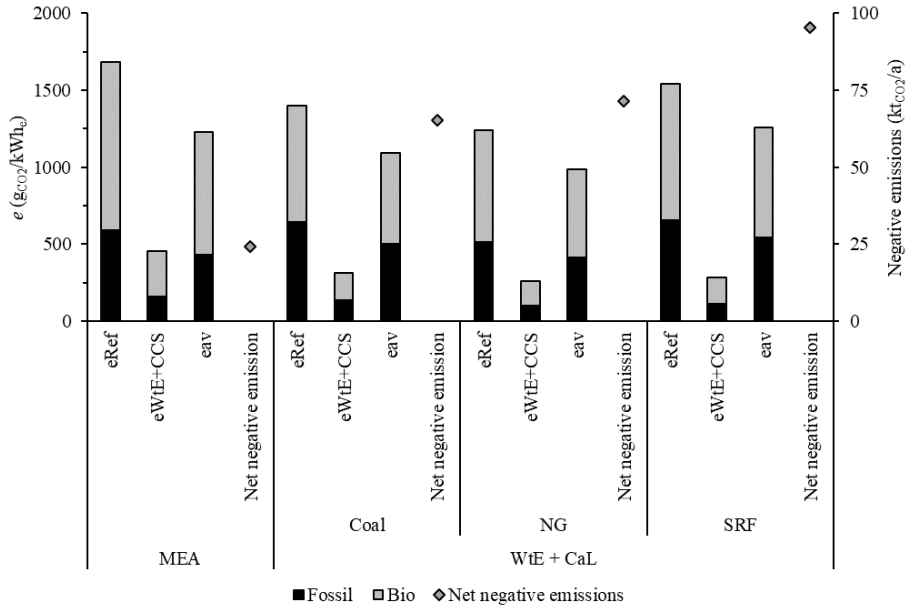

Figure 4: Specific CO_2 emissions w/o and w/ CCS and specific CO_2 avoidance for each CCS option.

3.2 Advanced CaL Heat Integration

Within this section, novel heat integration concepts (HIC) for the CaL excess heat integration into the existing WtE plant power cycle are proposed and discussed. External superheating and external reheating is a promising approach for efficiency improvements of WtE plants [69, 70]. In the present study, the sensible heat of the CO_2-depleted flue gas and of the CO_2-product at the outlet of carbonator and calciner are utilized as additional heat source for the steam cycle of the WtE plant, respectively. Figure 5 shows the heat integration concepts (left) and the integration of heat exchanger surfaces within the convective passes (right). Figure 5 a) shows the back-end case (HIC1) that is typically considered in CaL retrofitting scenarios. In the external superheating concept (HIC2), see Figure 5 b), excess heat from the CaL process is used to superheat the live steam in the host WtE power cycle. In another case (HIC3), excess heat from the CaL process is used to super- and reheat live steam within the WtE power cycle (see Figure 5 c). In each case, the thermal duty of the WtE boiler is kept constant. Along with the temperature, the live steam pressure was also raised. Practically, this implies modifications of

the existing WtE power cycle. Thus, an economic evaluation is not performed here, because of large uncertainties regarding the cost for the required modifications.

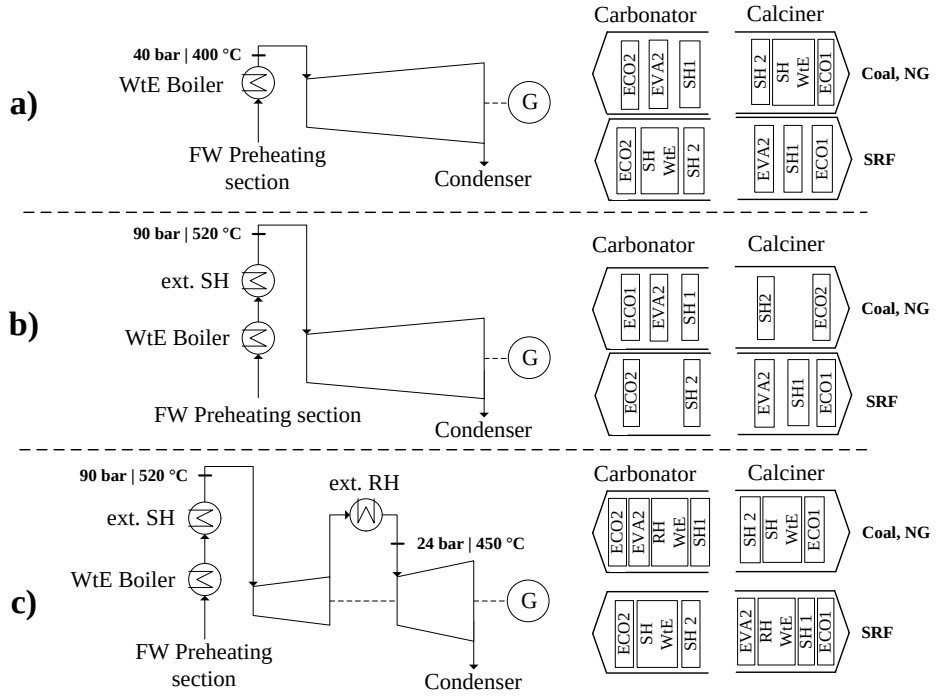

Figure 5: Heat integration concepts of CaL excess heat (left) and arrangement of CaL convective heat exchanger surfaces for the different fuel types (right). a) back-end (HIC1), b) external superheat (HIC2), c) external superheat + reheat (HIC3).

Table 2 summarizes the key results of the retrofitted WtE for the different heat integration options for each type of fuel. As a reference, the corresponding numbers of the back-end integration case are given. While increasing the heat integration level, the CaL gross electrical ratio decreases, whereas the overall net electrical efficiency increases. In all cases, the gain in net electrical efficiency accumulates to more than 5 %-points, for HIC3. Moreover it can be seen, that the major efficiency improvements are achieved due HIC2. The additional gain in the net electrical efficiency between HIC2 and HIC3 is limited to approximately 1 %-point.

Table 2: Key results of the CaL process for the different fuel and heat integration concepts.

HIC	Parameter	Unit	Coal	NG	SRF
1 (BE)	Gross power output	MW_e	32.7	31.5	35.1
	CaL gross power ratio	%	51.9	50.0	55.2
	Net power output	MW_e	19.6	20.3	21.1
	Net electrical efficiency	%	16.0	17.6	16.0
2 (SH)	Gross power output	MW_e	38.1	36.9	40.6
	CaL gross power ratio	%	39.7	37.7	43.4
	Net power output	MW_e	24.9	25.6	26.6
	Net electrical efficiency	%	20.3	22.0	20.3

3 (SH-RH)	Gross power output	MW_e	39.0	37.7	41.3
	CaL gross power ratio	%	35.9	33.8	39.9
	Net power output	MW_e	25.9	26.6	27.3
	Net electrical efficiency	%	21.2	23.0	20.8

3.3 Sensitivity study

In addition to tight heat integration, the effects of CaL process conditions and live steam parameter for the CaL power cycle are assessed. The boundaries for the sensitivity analysis are summarized in Table 15 (Appendix). The sensitivity parameters were chosen in order to address the most crucial assumptions made during the course of CaL process modelling. This is for instance the degree of sorbent deactivation, the oxygen concentration at the inlet and the outlet of the calciner, and the losses of fuel ash through the cyclones. All these parameters significantly influence the thermal requirement of the calciner, either directly as for the oxygen concentration or indirectly due to the higher make-up feed to compensate for the accumulation of fuel ash or forced sorbent deactivation. Additionally, transfer of sensible heat between the two major solid fluxes is applied in the best case. Moreover, three sets of live steam parameters for the CaL power cycles are investigated. In Figure 6, the net electrical efficiency depending on the CaL gross electrical ratio is shown for each heat integration concept while considering different CaL process conditions and different CaL power cycle live steam parameters. The results are presented for each type of fuel. Additionally, the net electrical efficiency of the WtE plant w/o CaL is indicated by a dashed line.

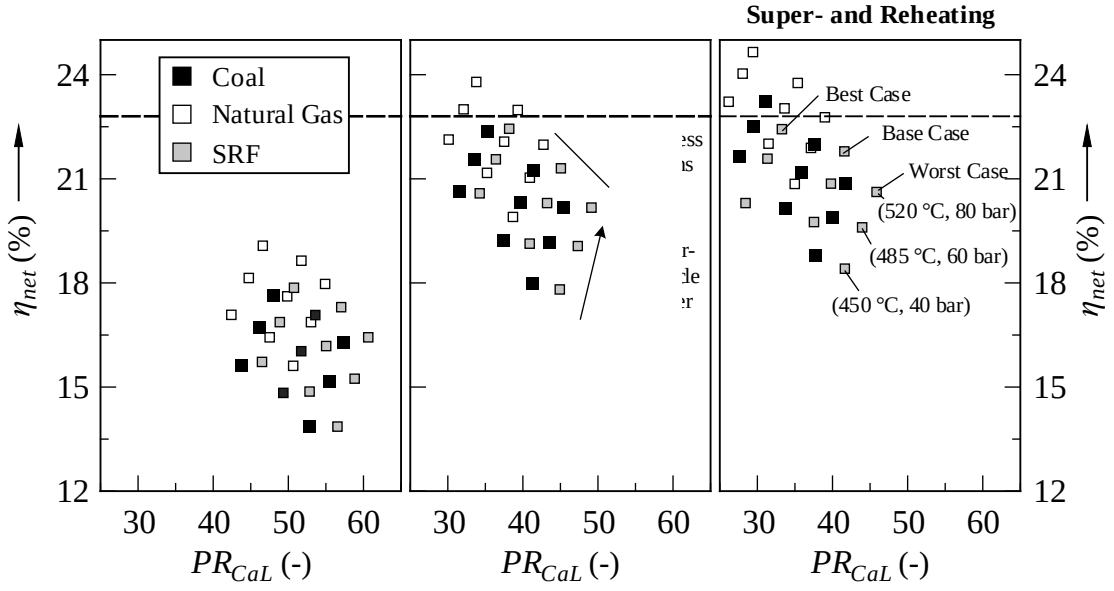

Figure 6: Results of the sensitivity analysis. Net electric efficiency and CaL gross power ratio depending on CaL-process conditions and CaL water-cycle steam parameters.

For the back-end case, the corresponding numbers for PR_{CaL} range from 40 to 65 %, whereas in the super- and reheating case, the CaL turbine delivers 25 to 50 % of the total gross power. At the same time, the net electrical efficiency increases if the WtE plant power cycle is upgraded by CaL excess heat. Thereby, the net electrical efficiency could be raised above the reference value. With improved CaL process conditions, less heat needs to be supplied to the calciner. Thus, less excess heat is available for steam generation. As a consequence, the share of the CaL turbine gross output is the lowest when assuming best CaL process conditions, respectively. On the other hand, the CaL gross electrical ratio increases along with higher steam parameters, due to a more efficient conversion of the recoverable excess heat.

4 Techno-Economic Analysis

Figure 7 shows the breakdown of LCOE and CAC for the WtE plant w/ and w/o CCS processes. For the CaL process, the back-end integration approach according to HIC1 is considered. For all CCS retrofit options, the LCOE increases considerably. This is mainly due to the fact that the reference WtE plant inherently has a low net electrical efficiency, especially compared to large-scale power generation systems. Thus, a relatively high amount of CO_2 needs to be captured per unit of electricity that is produced. Additionally, the size of the WtE plant is relatively small (P_{th} = 60 MW) compared to conventional power units (P_{th} > 500 MW), which are typically considered for CCS applications. Consequently, the benefits due to the economics of size are limited. This is especially the case of the reference MEA capture concept, which results in a very high LCOE (433 EUR/MWh$_e$) due to both, the power loss associated with the steam requirement for solvent regeneration, as well as the high capture investment and fixed operating costs. For the CaL based processes, the LCOE varies between 229 and 257 EUR/MWh$_e$ depending on the type of fuel that is considered. Among the different CO_2 capture options, the SRF-fueled CaL process allows for the lowest LCOE. In that case, the relatively low SRF price compensates for a higher efficiency penalty in comparison to the coal and NG options. The cost structure of the retrofitted CaL unit corresponds to the thermal size of the CaL process (see Table 1). Accordingly, the CAPEX of the NG case represents 33 % of the total LCOE. CAPEX of the coal and SRF case, accumulate to 36 and 42 %, respectively. The share of fixed OPEX costs (e.g. maintenance, insurance or labor cost) vary from 17 % (NG) up to 21 % (SRF). Even though, the utilization of NG allows for the best thermodynamic performance, the economics are worse due to the high fuel price that is responsible for almost 23.5 % of total LCOE.

As a result of the high LCOE increase, high CAC are obtained. While the CAC of the MEA-based capture results in costs as high as 288 EUR/$t_{CO2,av}$ the CAC of the CaL process vary between 119 and 183 EUR/$t_{CO2,av}$ depending on the type of fuel that is considered. Among these, the coal- and the NG-fueled CaL processes results in the highest costs due to the higher LCOEs but also due to the lower amount of specific avoided CO_2 emissions. In contrast, the economics of the SRF-fueled CaL process are significantly improved due the low SRF prices and due to the organic waste fractions, which results in additional negative CO_2 emissions.

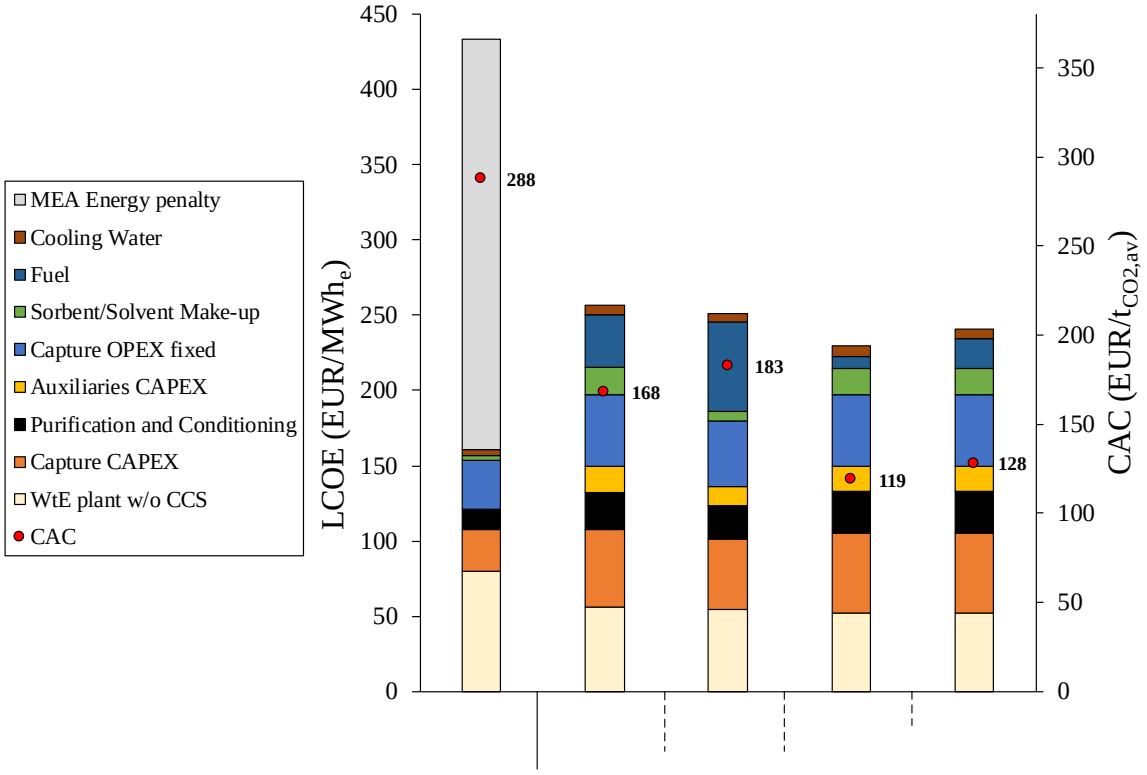

Figure 7: LCOE and CAC for the WtE plant w/ and w/o CO_2 capture processes.

While the costs presented above may seem high, it is important to realize that by considering CCS on a WtE plant, it enables a new business opportunity. In addition to the thermal treatment of wastes and the delivery of power and/or heat, the supply of negative CO_2 emissions represents another service of a CO_2 capture equipped WtE plant in the future perspective. In this regard, the economics of a CCS equipped WtE plant are valorized once CO_2 emission credits are sold to other market actors to compensate for their CO_2 emissions. In this case, the cost of delivering negative emissions would be same as the CAC. Even though, this cost range is still high compared to the current EU ETS price, they are on the lower range of estimates when compared to some of the other means considered to enable negative CO_2 emission such as BECCS and DAC. As shown in Figure 8 [3, 71-73], BECCS are expected to result in CAC between 50 to 250 EUR/t_{CO2},av and a WtE plant with SRF-based CaL is thus on the lower half

of these estimates. Furthermore, the WtE plant with CaL results in low CACs compared to DAC systems which are hoped to reach costs in the range of 100-200 EUR/t_{CO2},av [72] while they are current being sold for 980 EUR/$t_{CO2,av}$ [74]. Considering this aspect, CCS from WtE plants could be a cost-efficient solution to at the same time treat municipal waste in an environmentally friendly way, produce clean power, and enable a significant amount of the negative emissions required to meet the climate ambitions under the Paris agreement.

However, it is important to realize that the financial credit for the negative emissions may not be sufficient to fully compensate the cost of implementing CCS to capture both the non-biogenic and biogenic CO_2 emissions as shown in Figure 8. Indeed, even when the WtE plant can sell the negative CO_2 emissions for its CAC, the plant must compensate for the cost of avoiding its fossil emissions through higher electricity cost and/or higher fee charged to treat municipal waste in a climate-friendly way.

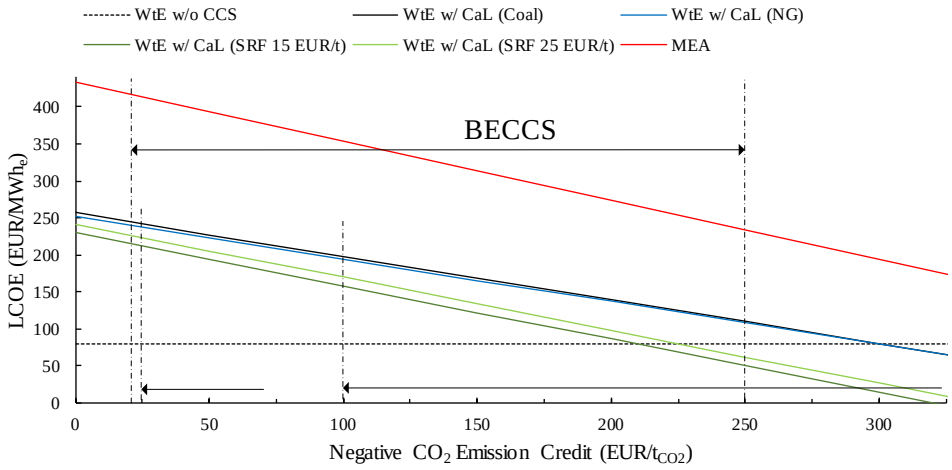

Figure 8: LCOE of the WtE plant w/o and w CCS processes dependent on the negative CO_2 emission credit.

5 Conclusions

A techno-economic analysis of a 60 MW_{th} WtE plant retrofitted by a CaL process for CO_2 capture was performed as part of this work. Based on a detailed process model for the CaL process, key process performance indicators such levelized cost of electricity and cost of CO_2 avoided were calculated. Investment costs were derived by a bottom-up approach based on the costs for each component. Moreover, the effects of the additional power supply by the CaL process were taken into account in the course of the techno-economic process evaluation, according to current state-of-the-art power plant performance characteristics. The techno-economic results were compared with a benchmark MEA scrubbing process. For the CaL process, three different types of supplementary fuel namely coal, NG and SRF were taken into

account. It was found, that for all CCS option, the LCOE increases significantly from 80 EUR/MWh_e (WtE plant w/o CCS) up to a range of 229 EUR/MWh_e (CaL-SRF) to 433 EUR/MWh_e (MEA). In contrast to large-scale CaL integration studies, the small thermal size of the WtE plant and low electrical efficiency of the reference WtE plant are the main cause for this increase. Corresponding numbers for the CAC range from 119 EUR/$t_{CO2,av}$ (CaL-SRF) up to 288 EUR/$t_{CO2,av.}$ (MEA). The CaL process for CO_2 capture involves installing a new power cycle associated with the CaL process where heat of carbonation and the oxy-fuel combustion of fuel in the calciner are used for power generation. This additional "power plant" has a higher efficiency that the WtE plant, thus improving the net electrical efficiency compared to the reference WtE plant. This is one of the main reasons that can be attributed to why the CaL process is competitive compared to MEA for CO_2 capture from WtE plants. Additionally, this work shows that WtE plants integrated CaL process for CO_2 capture can compete with BECCS and other technologies to provide cost-efficient negative emissions. In a sensitivity analysis, the influence of CaL process conditions and different CaL excess heat integration options were assessed. In case of a proper CaL excess heat integration into the existing WtE power cycle by means of external super- and reheating, the net electrical efficiency could be raised by more than 5 %-points compared to the reference WtE plant w/o CCS. CCS equipped WtE plants could be a cost-efficient solution to treat municipal waste in an environmentally friendly way, while at the same time, delivering clean power and negative CO_2 emissions.

Acknowledgements

The research leading to these results has received funding from the German Ministry of Economic Affairs and Energy based on a resolution of the German Parliament (MONIKA, FKZ: 03ET7089) and with support from the NCCS Centre, performed under the Norwegian research program Centers for Environment-friendly Energy Research (FME). The authors acknowledge the following partners for their contributions: Aker Solutions, Ansaldo Energia, CoorsTek Membrane Sciences, Emgs, Equinor, Gassco, Krohne, Larvik Shipping, Norcem, Norwegian Oil and Gas, Quad Geometrics, Shell, Total, Vår Energi, and the Research Council of Norway (257579/E20).

Appendix

Table 3: Composition and lower heating value of the solid fuels.

Parameter	Unit	MSW	Coal	SRF
$C_{organic}$	wt.%	18.8	0	15.2
C_{fossil}	wt.%	10.1	66.5	22.8
H	wt.%	3.20	3.87	3.78
N	wt.%	0.50	1.56	0.97
S	wt.%	0.10	0.52	0.29
O	wt.%	23.1	5.46	19.93
Cl	wt.%	0.40	0.01	0.74
H_2O	wt.%	25.0	8.00	19.4
Ash	wt.%	18.8	14.2	15.4
LHV	MJ/kg	10.0	25.2	15.7

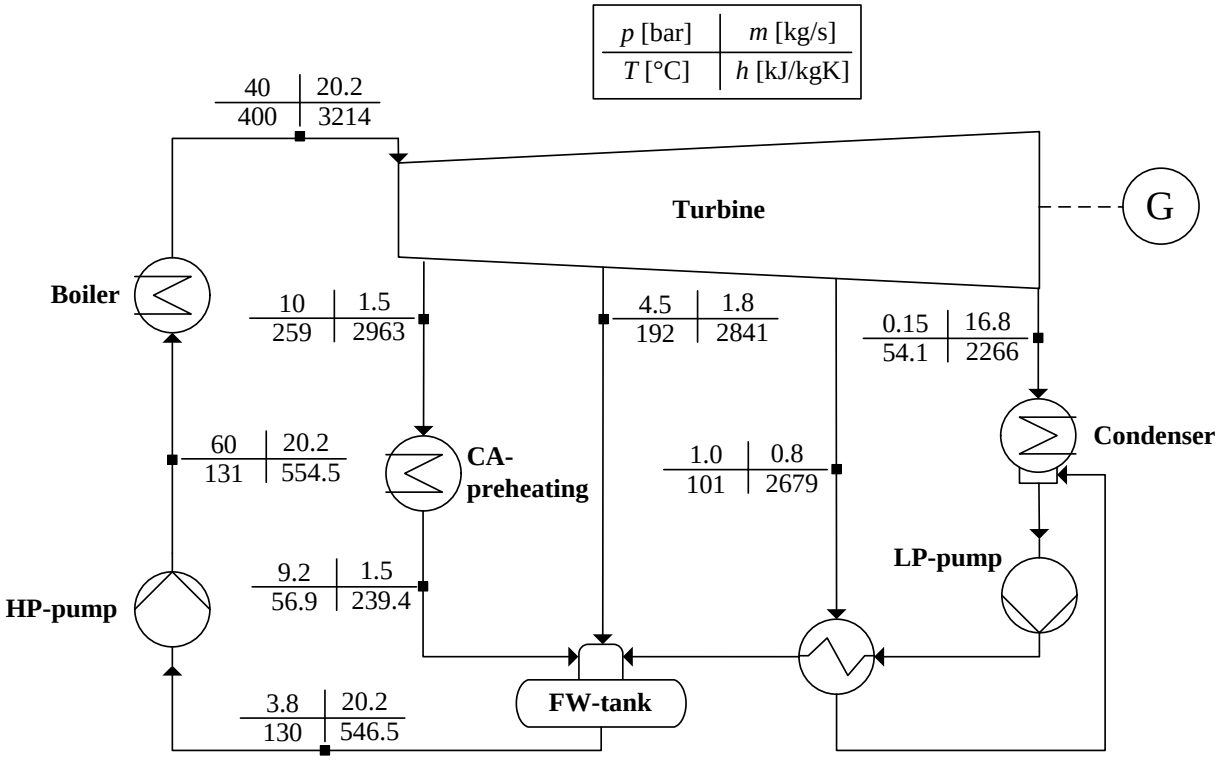

Figure 9: Thermodynamic power cycle layout of the reference WtE plant.

Table 4: Boundary conditions of the reference WtE plant.

Parameter	Unit	Value
Thermal input	MW_{th}	60.0
Boiler efficiency	%	61.7
Turbine isentropic efficiency	%	75.0
Turbine mechanical efficiency	%	94.0
Gross power output	MW_e	15.7
Gross electrical efficiency	%	26.2
Net power output	MW_e	13.6
Net electrical efficiency	%	22.4
Preheating temperature combustion air	°C	150
O_2 concentration at boiler exit	vol.%	6.07
O_2 concentration at stack	vol.%	8.23
Flue gas mass flow	kg/s	41.7
Flue gas temperature at stack	°C	135

Table 5: Composition of WtE flue gas at the stack.

Species	CO_2	N_2	H_2O	O_2	SO_2	HCl
Unit	vol.%	vol.%	vol.%	vol.%	ppm_v	ppm_v
Value	10.0	70.3	11.4	8.2	19.0	6.8

Table 6: Composition and lower heating value of natural gas.

Parameter	Unit	Value
CH_4	vol.%	89.1
C_2H_6	vol.%	7.00
C_3H_8	vol.%	1.00
CO_2	vol.%	2.00
N_2	vol.%	0.90
S	ppm_v	< 5
LHV	MJ/kg	46.5

Table 7: Boundary conditions for CaL process modelling.

Stream	Parameter	Unit	Value
Carbonator	Operating temperature	°C	650
	Specific solid inventory	kg/m²	1000
	Superficial gas velocity	m/s	5
	Height diameter ratio	-	3
	Outlet temperature of CO_2-depleted flue gas	°C	120
	Pressure drop	mbar	220
	Specific sorbent circulation rate	-	10
	CO_2 absorption efficiency	%	80
Calciner	Operating temperature	°C	900
	Superficial gas velocity	m/s	5
	Height diameter ratio	-	3
	Oxygen concentration at the inlet	vol.%	60
	Oxygen concentration at the outlet	vol.%	3.5
	Temperature recirculation gas	°C	200
	Pressure drop	mbar	160
	Outlet temperature off-gas	°C	120
Global	Fuel ash losses (coal)	%	60
	Fuel ash losses (SRF)	%	30
	Fan isentropic efficiency	%	85
	Fan mechanical efficiency	%	95
CaL Heat recovery system	Turbine isentropic efficiency	%	78
	Turbine mechanical efficiency	%	97
	Live steam temperature	°C	485
	Live steam pressure turbine inlet	bar	60
	Pressure drop SH, including turbine inlet valve	%	10
	Pump efficiency	%	80
	Gas phase pressure drop convective pass	mbar	35
	Evaporator pressure drop	bar	20
	Condenser pressure	bar	0.07
ASU	Oxygen purity	vol.%	95
	Specific power consumption	kWh/kg	220

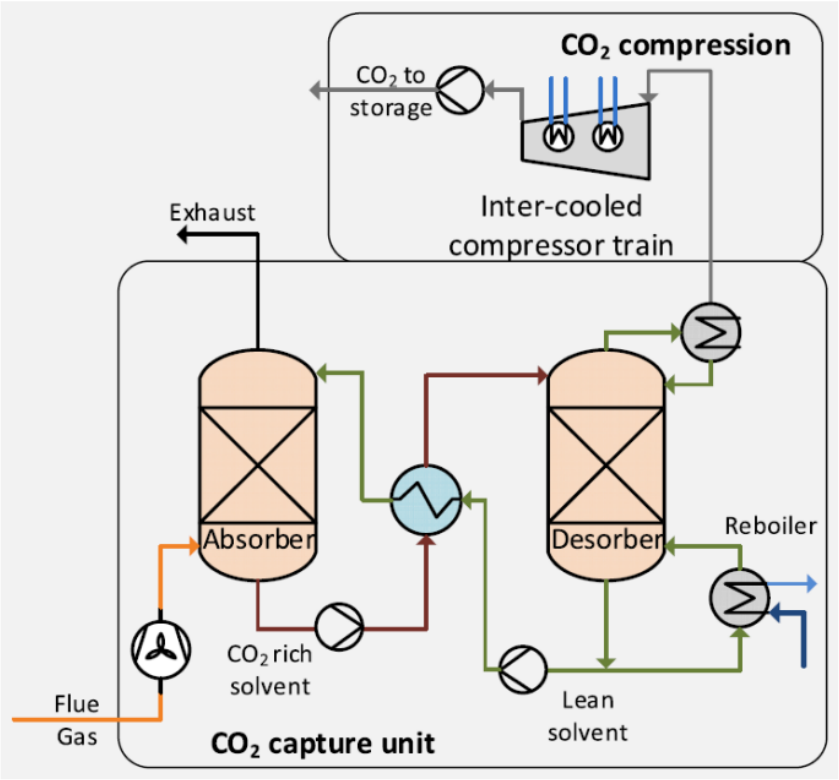

Figure 10: Principle of the MEA absorption process.

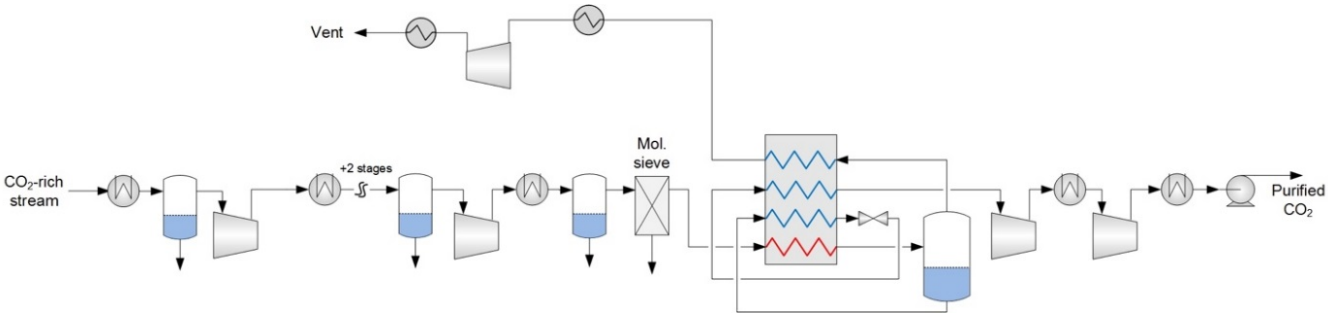

Figure 11: Schematic of single stage flash process CO_2 processing unit.

Table 8: Direct cost methodology for the evaluation of non-standard components.

Non-standard component	Direct cost model (k€$_{2017}$)	Source
Carbonator	$474 \cdot \text{Transferred thermal power [MW}_{th}\text{]} + 8\,360 \cdot \left(\frac{\text{Internal diameter [m]}}{4.7}\right)^{0.6}$	Modified[3] from [75]
Calciner	$415.3 \cdot (Fuel\ thermal\ input\ [MW_{th}])^{0.65}$	[75]
Heat recovery and steam production system	$26\,875 \cdot \left(\frac{Overall\ heat\ recovery\ duty\ [MW]}{266}\right)^{0.67}$	[64]
Sealed fan (T≤400ºC & P≤500kW)	$63 \cdot \left(\frac{Volumetric\ flow\ rate\ [m^3/h]}{25\,000}\right)^{0.5} + 39 \cdot \left(\frac{Power\ [kW]}{75}\right)^{0.65}$	[75]
Sealed fan (T≤400ºC & P>500kW)	$518 \cdot \left(\frac{Volumetric\ flow\ rate\ [m^3/h]}{25\,000}\right)^{0.5} + 303 \cdot \left(\frac{Power\ [kW]}{75}\right)^{0.65}$	[75]
Air separation unit	$63\,645 \cdot \left(\frac{Mass\ flow\ of\ oxygen\ [t_{O_2}/d]}{2\,717}\right)^{0.6}$	[75]
HCl removal unit	$-3.69 \cdot 10^{-7} \times (\text{Power output [MW]})^4 + 6.64 \cdot 10^{-4} \times \text{Power output}^3$ $-4.66 \cdot 10^{-1} \times \text{Power output}^2 + 133 \times \text{Power output}$	Regressed from [76]

Table 9**:** Cost of utilities.

Utilities	Unit	Cost	Reference
Coal	EUR/GJ$_{th}$	3	[64]
Natural gas	EUR/GJ$_{th}$	6	[64]
SRF	EUR/t	15 ;25	[68]
Limestone	EUR/t	30	[75]
MEA	EUR/t	1425	[65]
Cooling water	EUR/m^3	0.04	[65]

Table 10**:** Techno-economic boundary conditions for state-of-the-art power units.

Parameter	Unit	Coal	Gas	SRF
Net electrical efficiency	%	45.5	58.3	25.0
Total specific CO_2 emissions	g$_{CO2}$/kWh$_e$	763	352	1285
Fossil specific CO_2 emissions	g$_{CO2}$/kWh$_e$	763	352	771
Biogenic specific CO_2 emissions	g$_{CO2}$/kWh$_e$	0	0	514
LCOE	EUR/MWh$_e$	58.3	54.2	80

[3] Modified to include the impact of the carbonator diameter on cost

Table 11: Mass balance for the case WtE+CaL (coal).

Str .No.	$\dot{m}$	T	x_{vap}	Molar fraction (-)				Mass fraction (-)				
	kg/s	°C	-	CO_2	H_2	N_2	O_2	CaO	$CaCO_3$	$CaSO_4$	Ash	Coal
10	41.7	135	1.00	0.10	0.12	0.70	0.08	-	-	-	-	-
11	36.6	650	1.00	0.02	0.13	0.76	0.09	-	-	-	-	-
12	36.6	166	1.00	0.02	0.13	0.76	0.09	-	-	-	-	-
13	36.6	120	1.00	0.02	0.13	0.76	0.09	-	-	-	-	-
20	5.72	25.0	1.00	0.0	0.0	0.05	0.95	-	-	-	-	-
21	10.0	280	1.00	0.30	0.06	0.02	0.60	-	-	-	-	-
22	18.7	900	1.00	0.78	0.16	0.02	0.04	-	-	-	-	-
23	18.7	200	1.00	0.78	0.16	0.02	0.04	-	-	-	-	-
24	4.33	217	1.00	0.78	0.16	0.02	0.04	-	-	-	-	-
25	14.4	120	1.00	0.78	0.16	0.02	0.04	-	-	-	-	-
30	17.8	42.0	0.00	0.00	100	0.00	0.00	-	-	-	-	-
31	17.8	42.1	0.00	0.00	100	0.00	0.00	-	-	-	-	-
32	17.8	80.9	0.00	0.00	100	0.00	0.00	-	-	-	-	-
33	17.8	263	0.00	0.00	100	0.00	0.00	-	-	-	-	-
34	17.8	288	1.00	0.00	100	0.00	0.00	-	-	-	-	-
35	17.8	485	1.00	0.00	100	0.00	0.00	-	-	-	-	-
36	17.8	42.0	0.93	0.00	100	0.00	0.00	-	-	-	-	-
40	3.41	25.0	-	-	-	-	-	0.00	100	0.00	0.00	0.00
41	2.47	25.0	-	-	-	-	-	0.00	0.00	0.00	0.00	100
42	89.6	900	-	-	-	-	-	90.5	0.00	2.82	6.72	0.00
43	94.7	650	-	-	-	-	-	78.8	12.2	2.67	6.36	0.00
44	2.09	50.0	-	-	-	-	-	90.5	0.00	2.82	6.72	0.00

Table 12: Mass balance for the case WtE+CaL (natural gas).

Stream	$\dot{m}$	T	x_{vap}	Molar fraction (-)					Mass fraction (%)			
	kg/s	°C	-	CO_2	H_2O	N_2	O_2	NG	CaO	$CaCO_3$	$CaSO_4$	Ash
10	41.7	135	1.00	0.10	0.12	0.70	0.08	0.00	-	-	-	-
11	36.6	650	1.00	0.02	0.13	0.76	0.09	0.00	-	-	-	-
12	36.6	162	1.00	0.02	0.13	0.76	0.09	0.00	-	-	-	-
13	36.6	120	1.00	0.02	0.13	0.76	0.09	0.00	-	-	-	-
20	5.08	25.0	1.00	0.00	0.00	0.05	0.95	0.00	-	-	-	-
21	8.37	180	1.00	0.21	0.15	0.02	0.60	0.00	-	-	-	-
22	15.2	900	1.00	0.56	0.38	0.01	0.04	0.00	-	-	-	-
23	15.2	200	1.00	0.56	0.38	0.01	0.04	0.00	-	-	-	-
24	3.29	217	1.00	0.56	0.38	0.01	0.04	0.00	-	-	-	-
25	11.9	120	1.00	0.56	0.38	0.01	0.04	0.00	-	-	-	-
30	16.5	42.0	0.00	0.00	1.00	0.00	0.00	0.00	-	-	-	-
31	16.5	42.1	0.00	0.00	1.00	0.00	0.00	0.00	-	-	-	-
32	16.5	80.9	0.00	0.00	1.00	0.00	0.00	0.00	-	-	-	-
33	16.5	257	0.00	0.00	1.00	0.00	0.00	0.00	-	-	-	-
34	16.5	288	1.00	0.00	1.00	0.00	0.00	0.00	-	-	-	-
35	16.5	485	1.00	0.00	1.00	0.00	0.00	0.00	-	-	-	-
36	16.5	42.0	0.93	0.00	1.00	0.00	0.00	0.00	-	-	-	-
40	3.41	25.0	-	-	-	-	-		0.00	100	0.00	0.00
41	2.47	25.0	0.00	0.00	0.00	0.00	0.00	100	0.00	0.00	0.00	0.00
42	89.6	900	-	-	-	-	-		90.5	0.00	2.82	6.72
43	94.7	650	-	-	-	-	-		78.8	12.2	2.67	6.36
44	2.09	50.0	-	-	-	-	-		90.5	0.00	2.82	6.72

Table 13: Mass balance for the case WtE+CaL (SRF).

Stream	$\dot{m}$	T	x_{vap}	Molar fraction (-)				Mass fraction (%)				
	kg/s	°C	-	CO_2	H_2O	N_2	O_2	CaO	$CaCO_3$	$CaSO_4$	Ash	SRF
10	41.7	135	1.00	0.10	0.12	0.70	0.08	-	-	-	-	-
11	36.6	650	1.00	0.02	0.13	0.76	0.09	-	-	-	-	-
12	36.6	168	1.00	0.02	0.13	0.76	0.09	-	-	-	-	-
13	36.6	120	1.00	0.02	0.13	0.76	0.09	-	-	-	-	-
20	6.55	25.0	1.00	0.00	0.00	0.05	0.95	-	-	-	-	-
21	10.9	288	1.00	0.23	0.13	0.02	0.60	-	-	-	-	-
22	21.3	900	1.00	0.60	0.34	0.01	0.04	-	-	-	-	-
23	21.3	200	1.00	0.60	0.34	0.01	0.04	-	-	-	-	-
24	4.36	217	1.00	0.60	0.34	0.01	0.04	-	-	-	-	-
25	16.9	120	1.00	0.60	0.34	0.01	0.04	-	-	-	-	-
30	20.4	42.0	0.00	0.00	1.00	0.00	0.00	-	-	-	-	-
31	20.4	42.1	0.00	0.00	1.00	0.00	0.00	-	-	-	-	-
32	20.4	80.9	0.00	0.00	1.00	0.00	0.00	-	-	-	-	-
33	20.4	273	0.00	0.00	1.00	0.00	0.00	-	-	-	-	-
34	20.4	288	1.00	0.00	1.00	0.00	0.00	-	-	-	-	-
35	20.4	485	1.00	0.00	1.00	0.00	0.00	-	-	-	-	-
36	20.4	42.0	0.93	0.00	1.00	0.00	0.00	-	-	-	-	-
40	3.44	25.0	-	-	-	-	-	0.00	100	0.00	0.00	0.00
41	4.57	25.0	-	-	-	-	-	0.00	0.00	0.00	0.00	100
42	105	900	-	-	-	-	-	77.5	0.00	2.45	20.1	0.00
43	110	650	-	-	-	-	-	68.0	10.5	2.34	19.2	0.00
44	2.46	50.0	-	-	-	-	-	77.5	0.00	2.45	20.1	0.00

Table 14: CO_2 flows in the CaL system (kg/s).

Parameter	Coal	NG	SRF
Total CO_2 formation WtE plant	6.36	6.36	6.36
Fossil	2.23	2.23	2.23
Biogenic	4.14	4.14	4.14
Total CO_2 formation calciner (Fuel)	6.02	2.97	6.39
Fossil	6.02	2.97	3.83
Biogenic	0	0	2.55
Total CO_2 formation calciner (Limestone)	1.50	0.57	1.51
Fossil	1.50	0.57	1.51
Biogenic	0	0	0
Total CO_2 formation WtE plant + CaL process	13.9	9.90	14.3
Fossil	9.75	5.77	7.75
Biogenic	4.14	4.14	6.69
Total CO_2 captured	12.2	8.44	12.6
Fossil	8.99	5.21	6.91
Biogenic	3.20	3.24	5.69
Total CO_2 emission	1.69	1.46	1.66
Fossil	0.75	0.56	0.66
Biogenic	0.94	0.90	1.00
Net CO_2 emission	-2.44	-2.68	-5.03

Table 15: Boundary conditions for the sensitivity analysis.

Parameter	Unit	Worst case	Base Case	Best case
Sorbent residual conversion, X_r	-	0.060	0.075	0.090
Sorbent decay constant, k	-	0.624	0.520	0.416
O2-conc. at calciner inlet	vol.%	40	60	80
O2-conc. at calciner outlet	vol.%	4.5	3.5	2.5
Fuel ash losses (coal)	%	50	60	70
Fuel ash losses (SRF)	%	20	30	40
CaL Turbine isentropic efficiency	%	75	78	81
CaL live steam temperature	°C	450	485	520
CaL live steam pressure	bar	40	60	80
ASU specific power consumption	kWh_e/t_{O2}	240	220	200

6 References

[1] Gasser, T., et al., 2015. Negative emissions physically needed to keep global warming below 2 °C. Nat. Commun. 6, 7958. https://doi.org/10.1038/ncomms8958.

[2] Gambhir, A., et al., 2019. Energy systems changes in 1.5 °C, well below 2°C and 2°C scenarios. Energy Strategy Rev. 23, 69-80. https://doi.org/10.1016/j.esr.2018.12.006.

[3] Fasihi, M., et al., 2019. Techno-economic assessment of CO_2 direct air capture plants. J Clean. Prod. 224, 957-980. https://doi.org/10.1016/j.jclepro.2019.03.086.

[4] Sanz-Perez, E.S., et al., 2016. Direct Capture of CO_2 from Ambient Air. Chem. Rev. 116, 11840-11876. https://doi.org/10.1021/acs.chemrev.6b00173.

[5] Pires, J.C.M., 2019. Negative emissions technologies: A complementary solution for climate change mitigation. Sci. Total Environ. 672, 502-514. https://doi.org/10.1016/j.scitotenv.2019.04.004.

[6] Gough, C., 2018. Biomass Energy with Carbon Capture and Storage (BECCS), Unlocking Negative Emissions. first ed. John Wiley & Sons, Inc. 111 River Street, Hoboken, NJ 07030, USA.

[7] Creutzig, F., et al., 2015. Bioenergy and climate change mitigation: an assessment. Glob. Change Biol. Bioenergy 7, 916-944. https://doi.org/10.1111/gcbb.12205.

[8] Rolfe, A., et al., 2018. Integration of the calcium carbonate looping process into an existing pulverized coal-fired power plant for CO_2 capture: Techno-economic and environmental evaluation. Appl. Energy 222, 169-179. https://doi.org/10.1016/j.apenergy.2018.03.160.

[9] Singh, B., 2011. Comparative life cycle environmental assessment of CCS technologies. Int. J. Greenh. Gas Control 5, 911-921. https://doi.org/10.1016/j.ijggc.2011.03.012.

[10] Hoornweg, D., Bhada-Tata, P., 2012. What a Waste, A Global Review of Solid Waste Management. Urban Development & Local Government Unit, World Bank, Washington, DC 20433 USA.

[11] Brunner, P.H., Rechberger, H., 2015. Waste to energy - key element for sustainable waste management. Waste Manage. 37, 3-12. http://dx.doi.org/10.1016/j.wasman.2014.02.003.

[12] Eurostat, 2019. Municipal waste landfilled, incinerated, recycled and composted, EU-28, 1995-2017.png. 2019; Available from: https://ec.europa.eu/eurostat/statistics-explained/index.php?title=File:Municipal_waste_landfilled,_incinerated,_recycled_and_composted,_EU-28,_1995-2017.png.

[13] D. C. Wilson, 2015. Global Waste Management Outlook. International Solid Waste Association General Secretariat, Vienna, Austria.

[14] JOINT RESEARCH CENTRE Directorate B – Growth and Innovation Circular Economy and Industrial Leadership Unit European IPPC Bureau, 2018. Best Available Techniques (BAT) Reference Document for Waste Incineration - Final Draft, E.C.J.R. Centre.

[15] Viklund, P., et al., 2013. Corrosion of superheater materials in a waste-to-energy plant. Fuel process. Technol. 105, 106-112. https://doi.org/10.1016/j.fuproc.2011.06.017.

[16] Nielsen, H.P., et al., 2000. The implications of chlorine-associated corrosion on the operation of biomass-fired boilers. Prog. Energy Comb. Sci. 26, 283-298. https://doi.org/10.1016/S0360-1285(00)00003-4.

[17] Lombardi, L., et al., 2015. A review of technologies and performance of thermal treatment systems for energy recovery from waste. Waste Manage. 37, 26-44. http://dx.doi.org/10.1016/j.wasman.2014.11.010.

[18] Dong, J., et al., 2018. Comparison of waste-to-energy technologies of gasification and incineration using life cycle assessment: Case studies in Finland, France and China. J. Cleaner Prod. 203, 287-300. https://doi.org/10.1016/j.jclepro.2018.08.139.

[19] Di Lonardo, M.C., et al., 2016. The application of SRF vs. RDF classification and specifications to the material flows of two mechanical-biological treatment plants of Rome: Comparison and implications. Waste Manage. 47, 195-205. http://dx.doi.org/10.1016/j.wasman.2015.07.018.

[20] Flamme, S.,Geiping, J., 2012. Quality standards and requirements for solid recovered fuels: a review. Waste Manage. Res. 30, 335-353. http://dx.doi.org/10.1177/0734242X12440481.

[21] Haaf, M., et al., 2019. Techno-economic assessment of alternative fuels in second-generation carbon capture and storage processes. Mitig. Adapt. Strateg. Glob. Change. https://doi.org/10.1007/s11027-019-09850-z.

[22] Heck, V., et al., 2018. Biomass-based negative emissions difficult to reconcile with planetary boundaries. Nat. Climate Change 8, 151-155. https://doi.org/10.1038/s41558-017-0064-y.

[23] Pour, N., et al., 2018. Potential for using municipal waste as a resource for bioenergy with carbon capture and storage (BECCS). Int. J. Greenh. Gas Control 68, 1-15. https://doi.org/10.1016/j.ijggc.2017.11.007.

[24] Shimizu, T., et al., 1999. A twin fluid-bed Reactor for Removal of CO_2 from Combustion Processes. Chem. Eng. Res. Des. 77, 62-68. https://doi.org/10.1205/026387699525882.

[25] Abanades, J.C., et al., 2015. Emerging CO_2 capture systems. Int. J. Greenh. Gas Control 40, 126-166. https://doi.org/10.1016/j.ijggc.2015.04.018.

[26] Abanades, J.C., 2002. The maximum capture efficiency of CO_2 using a carbonation/calcination cycle of $CaO/CaCO_3$. Chem. Eng. J. 90, 303-306. https://doi.org/10.1016/S1385-8947(02)00126-2.

[27] Charitos, A., et al., 2010. Parametric investigation of the calcium looping process for CO_2 capture in a 10 kW_{th} dual fluidized bed. Int. J. Greenh. Gas Control 4, 776-784. https://doi.org/10.1016/j.ijggc.2010.04.009.

[28] Fan, F., et al., 2009. Continuous CO_2 capture from flue gases using a dual fluidized bed reactor with calcium-based sorbent. Ind. Eng. Chem. Res. 48, 11140-11147. https://doi.org/10.1021/ie901128r.

[29] Hughes, R.W., et al., 2005. Design, process simulation and construction of an atmospheric dual fluidized bed combustion system for in situ CO_2 capture using high-temperature sorbents. Fuel Process. Technol. 86, 1523-1531. https://doi.org/10.1016/j.fuproc.2005.01.006.

[30] Reitz, M., et al., 2016. Design and operation of a 300 kW_{th} indirectly heated carbonate looping pilot plant. Int. J. Greenh. Gas Control 54, 272-281. http://dx.doi.org/10.1016/j.ijggc.2016.09.016.

[31] Hilz, J., et al., 2017. Long-term pilot testing of the carbonate looping process in 1 MW_{th} scale. Fuel 210, 892-899. http://dx.doi.org/10.1016/j.fuel.2017.08.105.

[32] Hilz, J., et al., 2018. Investigation of the fuel influence on the carbonate looping process in 1 MW_{th} scale. Fuel Process. Technol. 169, 170-177. http://dx.doi.org/10.1016/j.fuproc.2017.09.016.

[33] Haaf, M., et al., 2019. Combustion of Solid Recovered Fuels within the Calcium Looping Process - Experimental Demonstration at 1 MW_{th} Scale. Exp. Therm. Fluid Sci. https://doi.org/10.1016/j.expthermflusci.2019.110023.

[34] Haaf, M., et al., 2019. Operation of a 1 MW_{th} Calcium Looping Pilot Plant Firing Waste-Derived Fuels in the Calciner. Powder Technol. Submitted.

[35] Arias, B., et al., 2018. Calcium looping performance under extreme oxy-fuel combustion conditions in the calciner. Fuel 222, 711-717. https://doi.org/10.1016/j.fuel.2018.02.163.
[36] Ming-Hui, C., et al., 2014. Design and Experimental Testing of a 1.9 MW_{th} Calcium Looping Pilot Plant. Energy Proc. 63, 2100-2108. https://doi.org/10.1016/j.egypro.2014.11.226.
[37] Martínez, I., et al., 2016. Review and research needs of Ca-Looping systems modelling for post-combustion CO_2 capture applications. Int. J. Greenh. Gas Control 50, 271-304. http://dx.doi.org/10.1016/j.ijggc.2016.04.002.
[38] Lasheras, A., et al., 2011. Carbonate looping process simulation using 1D fluidized bed model for the carbonator. Int. J. Greenh. Gas Control 5, 686-693. https://doi.org/10.1016/j.ijggc.2011.01.005.
[39] Vorrias, I., et al., 2013. Calcium looping for CO_2 capture from a lignite fired power plant. Fuel 113, 826-836. https://doi.org/10.1016/j.fuel.2012.12.087.
[40] Martinez, I., et al., 2011. Integration of a Ca Looping System for CO_2 capture in Existing Power Plants. AlChE J. 57, 2599-2607. https://doi.org/10.1002/aic.12461.
[41] Hanak, D.P., Manovic, V., 2017. Calcium looping combustion for high-efficiency low-emission power generation. J. Cleaner Prod. 161, 245-255. http://dx.doi.org/10.1016/j.jclepro.2017.05.080.
[42] Kunii, D., Levenspiel, O., 2000. The K-L reactor model for circulating fluidized beds. Chem. Eng. Sci. 55, 4563-4570. https://doi.org/10.1016/S0009-2509(00)00073-7.
[43] Kunii, D., Levenspiel, O., 1991. Fluidization Engineering, sec ed. Butterworth-Heinemann, Newton.
[44] Kunii, D., Levenspiel, O., 1997. Circulating fluidized-bed reactors. Chem. Eng. Sci. 52, 2471-2482. https://doi.org/10.1016/S0009-2509(97)00066-3.
[45] Geldart, D., et al., 1979. Effect of fines on entrainment from gas fluidized beds. Trans. Inst. Chem. Eng. 57, 269-275.
[46] Romano, M.C., 2012. Modeling the carbonator of a Ca-looping process for CO_2 capture from power plant flue gas. Chem. Eng. Sci. 69, 257-269. https://doi.org/10.1016/j.ces.2011.10.041.
[47] Charitos, A., et al., 2011. Experimental Validation of the Calcium Looping CO2 Capture Process with Two Circulating Fluidized Bed Carbonator Reactors. Ind. Eng. Chem. Res 50(16), 9685-9695. https://doi.org/10.1021/ie200579f.
[48] Grasa, G.S., Abanades, J.C., 2006. CO_2 Capture Capacity of CaO in Long Series of Carbonation/Calcination Cycles. Ind. Eng. Chem. Res. 45, 8846-8851. https://doi.org/10.1021/ie0606946.
[49] Sun, P., et al., 2007. Removal of CO_2 by Calcium-Based Sorbents in the Presence of SO_2. Energy Fuels 21, 163-170. https://doi.org/10.1021/ef060329r.
[50] Stanmore, B.R., Gilot, P., 2005. Review-calcination and carbonation of limestone during thermal cycling for CO_2 sequestration. Fuel Process. Technol. 86, 1707-1743. https://doi.org/10.1016/j.fuproc.2005.01.023.
[51] Grasa, G.S., et al., 2008. Sulfation of CaO Particles in a Carbonation/Calcination Loop to capture CO_2. Ind. Eng. Chem. Res. 47, 1630-1635. https://doi.org/10.1021/ie070937+.
[52] Rodrìguez, N., et al., 2010. Average activity of CaO particles in a calcium looping system. Chem. Eng. J. 156, 388–394. https://doi.org/10.1016/j.cej.2009.10.055.
[53] Bhatia, S.K., Perlmutter, D.D., 1983. Effect of the Product Layer on the Kinetics of the CO_2-Lime Reaction. AlChE J. 29, 79-86. https://doi.org/10.1002/aic.690290111.
[54] R. Anantharaman, et al., 2011. CESAR D 4.9 European best practice guideline for assessment of CO_2 capture technologies.

[55] R. Anantharaman, et al., 2017. CEMCAP D3.2 CEMCAP framework for comparative techno-economic analysis of CO_2 capture from cement plants.
[56] Mantripragada, H.C., et al., 2019. Boundary Dam or Petra Nova - Which is a better model for CCS energy supply. Int. J. Greenh. Gas Control 82, 59-68. https://doi.org/10.1016/j.ijggc.2019.01.004.
[57] Stephenne, K., 2014. Start-Up of World's First Commercial Post-Combustion Coal Fired CCS Project: Contribution of Shell Cansolv to SaskPower Boundary Dam ICCS Project. Energy Proc. 63, 6106-6110. https://doi.org/10.1016/j.egypro.2014.11.642.
[58] Lindqvist, K., et al., 2014. Integration aspects of reactive absorption for post-combustion CO_2 capture from NGCC (natural gas combined cycle) power plants. Energy 78, 758-767. http://dx.doi.org/10.1016/j.energy.2014.10.070.
[59] Chemical Engineering, Economic Indicators: Chemical Engineering Plant Cost Index (CEPCI). 2019.
[60] Trading Economics, Trading Economics database on Euro area inflation rate. 2018.
[61] ADEME, La valorisation énergétique des déchets par incinération. Available from: http://www.vernimmen.net/ftp/La_valorisation_energetique_des_dechets_par_incineration.pdf. 2011.
[62] ADEME, ENQUETE SUR LES PRIX DE L'INCINERATION DES DECHETS MUNICIPAUX. 2011.
[63] NETL, Quality guidelines for energy system studies: Cost estimation methodology for NETL assessments of power plant performance. DOE/NETL-2011/1455. 2011.
[64] R. Anantharaman, et al., 2011. DECARBit D 1.4.3 European best practice guidelines for assessment of CO_2 capture technologies.
[65] Gardarsdottir, S.O., et al., 2019. Comparison of Technologies for CO_2 Capture from Cement Production - Part 2: Cost Analysis. Energies 12, 542. https://doi.org/10.3390/en12030542.
[66] Roussanaly, S., et al., 2019. Techno-economic comparison of technologies for pre-combustion CO_2 capture from a lignite-fired IGCC. Front. Chem. Sci. Eng. https://doi.org/10.1007/s11705-019-1870-8.
[67] IEAGHG, 2017. Understanding the cost of retrofitting CO_2 capture in an integrated oil refinery. IEAGHG Technical Review 2017-TR8, August 2017. www.sintef.no/recap
[68] ADEME, Etat de l'art de la production et de l'utilisation de combustibles solides de recuperation. Available from: https://www.ademe.fr/sites/default/files/assets/documents/88363_etat-art-csr-rapport-final.pdf. 2012.
[69] Schu, R., Leithner, R. 2008. Waste to Energy - Higher Efficiency with External superheating. Second International Symposium on Energy from Biomass and Waste, Venice.
http://www.ecoenergy.de/go_public/freigegeben/Waste_to_energy_Schu_Leithner_Venice2008_Presentation.pdf.
[70] Becidan, M., Anantharaman, R. 2012. Dual-fuel Cycles to Increase the Efficiency of WtE Installations. Chem. Eng. Transact. 29, 727-732. https://doi.org/10.3303/CET1229122.
[71] Bhave, A., et al., 2017. Screening and techno-economic assessment of biomass-based power generation with CCS technologies to meet 2050 CO_2 targets. Appl. Energy 190, 481-489. https://doi.org/10.1016/j.apenergy.2016.12.120.
[72] Bui, M., et al., 2018. Carbon capture and storage (CCS): the way forward. Energy Environ. Sci. https://doi.org/10.1039/c7ee02342a.
[73] Martìnez, I., et al., 2018. CO_2 capture in existing power plants using second generation Ca-Looping systems firing biomass in the calciner. J. Cleaner Prod. 187(20), 638-649. https://doi.org/10.1016/j.jclepro.2018.03.189.

[74] Climeworks. Available from: https://climeworks.shop/. Cited: 08/11/2019.
[75] Cinti, G., et al., 2018. CEMCAP Deliverable D4.4 Cost of critical components in CO_2 capture processes. H2020 CEMCAP. 2018.
[76] United States Environmental Protection Agency, Documentation for EPA's Power Sector Modeling Platform v6 - November 2018 Reference Case. Available from: https://www.epa.gov/airmarkets/documentation-epas-power-sector-modeling-platform-v6-november-2018-reference-case. 2019.